Rare decay $t \to c\gamma\gamma$ via scalar leptoquark doublets

A. Bolaños-Carrera
Tecnologico de Monterrey, School of Engineering and Sciences, Avenida Eugenio Garza Sada 2501, CP 64849, Monterrey, Nuevo Leon, Mexico

R. Sánchez-Vélez*
Departamento de Física, Centro de Investigación y de Estudios Avanzados del IPN, Apartado Postal 14-740 07000 Ciudad de México, México

G. Tavares-Velasco
Facultad de Ciencias Físico Matemáticas, Benemérita Universidad Autónoma de Puebla, Apartado Postal 1152, Puebla, Puebla, México

(Received 3 December 2022; accepted 4 April 2023; published 12 May 2023)

A calculation of the one-loop contribution to the rare three-body flavor changing neutral current top quark decay $t \to c\gamma\gamma$ is presented in the framework of models with one or more scalar leptoquark (LQ) $SU(2)$ doublets with hypercharge $7/6$. Analytical expressions for the invariant amplitude of the generic decay $f_i \to f_j\gamma\gamma$, with $f_{i,j}$ a lepton or quark, are presented in terms of Passarino-Veltman integral coefficients, from which the amplitudes for the processes $t \to c\gamma\gamma$ and $\ell_i \to \ell_j\gamma\gamma$ follow easily. An analysis of the current constraints on the parameter space is presented in the scenario with only one scalar LQ doublet, and bounds on the LQ couplings are obtained from the muon $g-2$ anomaly, the lepton flavor violating decay $\tau \to \mu\gamma$ and extra constraints meant to avoid tension between theory predictions and experimental data. For a LQ with a mass in the range of 1–1.5 TeV, the estimate $\mathrm{Br}(t \to c\gamma\gamma) \sim 10^{-11}$–$10^{-12}$ is obtained for the largest allowed values of the LQ coupling constants, which means that this decay would be below the reach of future experimental measurements. We also consider a scenario with three scalar doublets, which was recently proposed to explain the lepton flavor universality violation anomalies in B decays as well as the muon $g-2$ anomaly. Although this scenario allows large LQ couplings to the tau lepton and the c and t quarks, the branching ratio of the $t \to c\gamma\gamma$ decay is also of the order of 10^{-11}–10^{-12} for LQ masses of the order of 1.7 TeV.

DOI: 10.1103/PhysRevD.107.095018

I. INTRODUCTION

The study of flavor changing neutral currents (FCNCs) has long been a topic of great interest both theoretically and experimentally [1,2]. This class of effects is considerably suppressed according to the standard model (SM), where they arise up to the one-loop level [3,4]. Therefore FCNC transitions could provide signals of new physics and shed light on any possible SM extension. On the experimental side, the advent of the large hadron collider (LHC) offers a great potential to search for signals of various rare FCNC top quark decays, such as $t \to cV$ ($V = \gamma, g, Z$), $t \to cH$, $t \to c\ell^-\ell^+$, $t \to c\gamma\gamma$, $t \to cgg$, $t \to c\gamma H$, and $t \to c\gamma Z$. While the two-body decays $t \to cV$ and $t \to cH$ have been largely studied in the context of the SM and several of its extensions [3,5–17], less attention has been paid to the three-body decays as they are expected to be more suppressed, but also because they involve lengthy and cumbersome calculations.

In the SM the decay $t \to c\gamma$ can only arise at the one-loop level due to electromagnetic gauge invariance and is further suppressed due to the Glashow-Iliopoulos-Maiani (GIM) mechanism, so its branching ratio is considerably small, of the order of 10^{-10} [3,4]. However, in SM extensions such a decay may not be GIM suppressed and its branching ratio $\mathrm{Br}(t \to c\gamma)$ can be enhanced by several orders of magnitude, ranging from values of the order of 10^{-7} in two-Higgs doublet models [3] up to 10^{-5} in supersymmetric models [9–12]. Furthermore, some time ago, it was pointed out that there are some new physics scenarios where the three-body

*Corresponding author.
ricsv05@icloud.com

decay $t \to c\gamma\gamma$ could have a larger branching ratio than those of the two-body decays $t \to c\gamma$ [18]. Thus, it is worth studying the rare three-body FCNC top quark decays in extension models despite the complexity involved in the respective calculation in order to assess if they could be at the reach of experimental detection. Along this line, the decay $t \to c\gamma\gamma$ has been studied in the framework of the little Higgs model with T parity [19,20] and also in a top-color assisted technicolor theory [21].

In this work we will present a calculation of the $t \to c\gamma\gamma$ decay in the framework of leptoquark (LQ) models. Two-body FCNC top quark decays have already been calculated in the context of this class of models: a calculation of the contribution of a model with an $SU(2)$ scalar LQ doublet to the two-body decays $t \to cX$ ($X = \gamma$, Z, H, g) and also to the three-body decay $t \to c\ell^-\ell^+$ was presented in Ref. [22] along with a comprehensive analysis of the parameter space of the model consistent with the then current constraints from direct LQ searches at the LHC, the Higgs boson coupling modifiers, the muon $g-2$ anomaly, and the lepton flavor violating decay (LFV) $\tau \to \mu\gamma$. To our knowledge there is no previous calculation of the contribution of LQs to the three-body FCNC top quark rare decay $t \to c\gamma\gamma$.

LQs are hypothetical particles carrying both lepton and color number that were proposed long ago in the Pati-Salam model [23] and also in the context of grand unification theories [24–29], though they can also arise naturally in theories with composite fermions [30–32], superstring-inspired E_6 models [33,34], technicolor models [35–37], etc. A shortcoming of some of these models is that they could allow dangerous LQ diquark couplings that would induce proton decay at the tree level [38], so additional symmetries must be invoked to preserve proton stability. In addition, if LQs couple to the first fermion generation, large contributions to low-energy observable quantities can arise, such as atomic parity violation, parity-violating electron scattering, coherent neutrino-nucleus scattering, and electroweak precision parameters, which together with direct searches at the LHC set tight constraints on the parameter space of such LQs [39–44]. However, LQ couplings to the second and third fermion families are not strongly constrained yet, and recently LQ particles have become the source of renewed attention in the literature (for a recent LQ review see Ref. [45]) since they could explain the lepton flavor universality violating (LFUV) effects hinted at semileptonic B decays and can also provide a solution to the muon $g-2$ anomaly [46–126]. Furthermore, LQs can be accommodated in models where neutrino mass is generated radiatively [84,98,101,125,125,127,128]. It is thus worth calculating LQ contributions to FCNC rare top quark decays.

The rest of the presentation is organized as follows. In Sec. II we present an overview of LQ models and focus on a minimal renormalizable scalar LQ model with no proton decay, where there are potential sources of flavor change in the quark sector induced by scalar LQs. Section III is devoted to discussing the calculation of the $t \to c\gamma\gamma$ decay amplitude in our LQ model: for the sake of completeness, the invariant amplitude for the general fermion decay $f_i \to f_j\gamma\gamma$ is obtained via the Passarino-Veltman reduction method, and the corresponding form factors are presented in Appendix A. From these expressions the decay width for the $t \to c\gamma\gamma$ process follows straightforwardly. The numerical analysis of the LQ parameter space consistent with the current experimental constraints, considering two potential scenarios for the LQ couplings along with the numerical evaluation of the $t \to c\gamma\gamma$ branching ratio are presented in Sec. IV. Finally, Sec. V is devoted to the conclusions and outlook.

II. A RENORMALIZABLE SCALAR LQ MODEL WITH PROTON STABILITY

We now present the theoretical framework required for the calculation of the rare top quark decay $t \to c\gamma\gamma$ focusing on a model where there is no dangerous contribution to proton decay. LQs are hypothetical particles carrying both lepton and color number, thereby coupling simultaneously to lepton and quarks. A systematic classification of all $SU(3)_C \times SU(2)_L \times U(1)_Y$ LQ representations and their renormalizable couplings to the SM fields was presented in Ref. [129] via effective Lagrangians. According to all possible representations of the SM gauge group, it was found that LQs can be accommodated in ten representations: five scalar ones and five vector ones.

As far as vector LQs are concerned, they arise in grand unification theories and may be troublesome as they can trigger rapid proton decay, which sets a lower constraint of 10^{16} GeV on the mass of such gauge LQs [25,38]. Even if an *ad-hoc* symmetry is imposed to forbid proton decay, the mass of vector LQs can be strongly constrained by rare K, π, and B meson decays [130,131]. However, there are two phenomenologically viable vector LQ models at the TeV scale with no proton decay, which involve the $(3,1,2/3)$ and $(3,3,2/3)$ vector LQ representations [132]. Models based on these representations have been studied recently as they can explain the LFUV anomalies in B-meson decays and still be consistent with current experimental constraints from K and B meson decays and electroweak precision observable parameters as well as direct searches at the LHC [53,57,59,60,60–62,70,73,79,133]. In particular, the $(3,1,2/3)$ vector LQ representation U_1^μ is attractive as it is predicted by the minimal realization of the Pati-Salam model [23] and also due to the absence of tree-level contributions to the very constrained decay $B \to K^*\nu\bar{\nu}$ [89,132].

As for scalar LQ models, there are two renormalizable scalar LQ models [134] that do not have proton decay at the tree level, which involve the $(3,2,7/6)$ and $(3,2,1/6)$ scalar LQ representations. For the purpose of this work, we are interested in LQ models with the scalar LQ $(3,2,7/6)$ representation, which is usually denoted as R_2 in the

literature [129]. This scalar $SU(2)$ LQ doublet representation provides simple renormalizable models that conserve baryon number [134], thereby forbidding dangerous contributions to proton decay. The phenomenology of LQ models with scalar doublets R_2 has been extensively studied in the literature: for representative works see for instance [22,44,47,50,53,78,82,90,103,114,115,117,118,121,123,124,126,134–153]. Such models have been the source of attention recently as can explain the apparent discrepancies between the SM predictions and experimental measurements. For instance, models with only one R_2 scalar LQ doublet can explain the muon anomaly and the R_{D,D^*} anomalies [115,117,126], though the authors of Ref. [154] showed that multiple R_2 scalar LQ doublets are necessary to explain the apparent R_{K,K^*} anomalies [155,156], which however seem to be excluded by the most recent measurements of the $b \to s\ell^+\ell^-$ decay by the LHCb collaboration [157]. In addition, another appealing feature of models with R_2 scalar LQ doublets is that they can provide a mechanism of neutrino mass generation, such as in the models studied in [84,98,127,128], where neutrinos' masses are generated via the mixing of R_2 with an extra LQ singlet S_1 through radiative corrections.

In this work we will consider LQ models where the SM is augmented with one or more $SU(2)$ scalar doublets R_2 that induce the FCNC decay $t \to c\gamma\gamma$. We will present the theoretical framework for a lone scalar doublet R_2, and the extension for models with multiple scalar LQ doublets R_2 will follow straightforwardly. As already mentioned, the presence of additional scalar LQ doublets R_2 is meant to explain the LFUV anomalies in b-hadron decays, though additional contributions to FCNC top quark decays are not necessarily expected since extra symmetries may be required to meet the current experimental constraints, thereby imposing tight constraints on the parameter space of the model.

The R_2 LQ doublet has hypercharge $7/6$, thereby giving rise to two scalar LQs with electric charges $2/3$ and $5/3$, which we denote by $\Omega_{2/3}$ and $\Omega_{5/3}$, where the subscripts stand for the LQ electric charge. Both $\Omega_{2/3}$ and $\Omega_{5/3}$ predict rich phenomenology as already noted and can give new contributions to several observable quantities (for a recent review of LQ constraints from experimental data see [45]), such as atomic parity violation [43,158], meson decays [39,41,43,45,130], electric dipole moments of leptons [134], LFV lepton decays [159,160], oscillations in K, D, and B meson systems [40,161], oblique corrections [162,163], electroweak precision observable parameters [164,165], Higgs boson modifiers [22,163], etc., which along with direct searches at the LHC [166–170] set strong constraints on the corresponding parameter space. For the purpose of this work we are interested in the charge $5/3$ LQ as it couples to left- and right-handed fermions simultaneously and can induce new physics effects in the LFV decays $H \to \mu\tau$ [140] and $\ell_i \to \ell_j\gamma$ [22,152,159,160] as well as the FCNC top quark decays $t \to c\gamma$, $t \to cZ$, and $t \to cH$ [22]. This LQ can also give contributions to the $t \to c\gamma\gamma$ decay, which is the topic of interest of the present work.

The Yukawa Lagrangian for an R_2 doublet can be written as

$$\mathcal{L}_{F=0} = Y^{RL}_{ij} R_2^T \bar{u}'^i_R i\tau_2 L'^j_L + Y^{LR}_{ij} \bar{Q}'^i_L e'^j_R R_2 + \text{H.c.}, \quad (1)$$

where as usual L'^i_L and Q'^i_L are $SU(2)_L$ left-handed lepton and quark doublets, respectively, whereas e'^i_R and q'^i_R are $SU(2)$ singlets, with i and j being generation indices. For the Yukawa couplings we use the notation of Refs. [154,171] and consider that the R_2 LQ only couples to the fermions of the second and third generations since the couplings to the fermions of the first generation are strongly constrained by low-energy data, such as atomic parity violation [39,43,158], universality in leptonic pion decays [39,40,43], μe conversion [41], flavor changing kaon decays [41,130], and $K^0 - \bar{K}^0$ and $D^0 - \bar{D}^0$ mixing [39,40,161]. For other recent analyses see [44,150].

After electroweak symmetry breaking we rotate the $SU(2)_L$ LQ doublet into its mass eigenstates: $R_2^T = (\Omega_{5/3}\Omega_{2/3})$, which at the lowest order in v coincide with the weak eigenstates [163]. As for the weak eigenstates of the up and down quarks, we will consider two scenarios. In the so-called up-aligned scenario, the weak eigenstates of the up quarks u'^i are chosen as the mass eigenstates u^i, whereas the weak eigenstates of the down quarks d'^i are rotated to the mass eigenstates d^i via the Cabibbo-Kobayashi-Maskawa mixing matrix V_{CKM}: $d'^i \to V^{ik}_{\text{CKM}} d^k$. In this scenario the LQ interactions with the SM fermions read as

$$\mathcal{L}_{F=0} = (Y^{RL}_{ij} \bar{u}^i P_L e^j + Y^{LR}_{ij} \bar{u}^i P_R e^j)\Omega_{5/3} + \hat{Y}^{LR}_{ij} \bar{d}^i P_R e^j \Omega_{2/3} - Y^{RL}_{ij} \bar{u}^i P_L \nu_j \Omega_{2/3} + \text{H.c.}, \quad (2)$$

where $P_{L,R}$ are the chiral projection operators and we define $\hat{Y}^{LR}_{ij} = V^{ik}_{\text{CKM}} Y^{LR}_{kj}$. Alternatively, in the down-aligned scenario one sets $d'^i = d^i$ and $u'^i = V^{ik}_{\text{CKM}} u^k$. This choice only affects the LQ interactions with left-handed up quarks, so the replacement $\bar{u}^i P_R e^j \Omega_{5/3} \leftrightarrow \bar{d}^i P_R e^j \Omega_{2/3}$ must be made in Eq. (2) to obtain the corresponding interaction Lagrangian.

Below we will analyze two LQ models (scenarios I and II), and constraints on LQ Yukawa couplings will be obtained from experimental data. In scenario I we consider a model with only one R_2 scalar LQ doublet that is not primarily meant to explain the LFUV anomalies in B-meson decays: the R_2 LQ doublet could be assumed as a piece of a more complete model provided with another mechanism to explain such anomalies, as long as they are confirmed by future measurements. In this scenario we do not assume a particular pattern for the LQ Yukawa couplings, which are then bounded from the muon $g-2$

anomaly, the LFV decay $\tau \to \mu\gamma$, and other experimental constraints. As far as scenario II is concerned, we consider the three-LQ-doublet model recently proposed to address the B-meson anomalies [154], which require that LFV is forbidden. In such a model, the down-aligned scenario was assumed, and a comprehensive analysis of the allowed regions of the parameter space of the model consistent with experimental constraints was performed [154]. We will not explore other alternative models with a specific structure for the LQ Yukawa couplings here as the two scenarios considered in our analysis will allow us to assess the order of magnitude of the branching ratio for the $t \to c\gamma\gamma$ decay.

As for the LQ couplings to the photon, they can be obtained from the kinetic Lagrangian

$$\mathcal{L}_{\text{kin}} = \frac{1}{2}(D_\mu R_2)^\dagger D^\mu R_2, \tag{3}$$

where the $SU(2)_L \times U(1)_Y$ covariant derivative is given by

$$D_\mu R_2 = \left(\partial_\mu + ig\frac{\tau^i}{2}W_\mu^i + ig'\frac{7}{6}B_\mu\right)R_2. \tag{4}$$

Thus, the LQ couplings to one and two photons can be simply written as

$$\begin{aligned}\mathcal{L}_{\text{kin}} \supset \sum_{Q=2/3,5/3} &(iq_Q A^\mu(\Omega_Q^*\partial_\mu\Omega_Q - \Omega_Q\partial_\mu\Omega_Q^*) \\ &+ q_Q^2 A_\mu A^\mu \Omega_Q^*\Omega_Q),\end{aligned} \tag{5}$$

where q_Q denotes the LQ electric charge. Finally, we consider the following renormalizable effective LQ interactions to the SM Higgs doublet Φ

$$\mathcal{L} = (M_{R_2}^2 + \lambda_{R_2}\Phi^\dagger\Phi)(R_2^\dagger R_2), \tag{6}$$

where M_{R_2} is the LQ mass matrix. After rotating to the mass eigenstates the LQ masses become nondegenerate at the lowest order in v^2. We can also obtain the Higgs boson coupling to the LQs:

$$\mathcal{L} \supset \sum_{Q=2/3,5/3} \lambda_{\Omega_Q} v H \Omega_Q^*\Omega_Q, \tag{7}$$

which can be useful to constrain the LQ couplings to the SM Higgs boson from the Higgs coupling modifiers κ_γ and κ_g [22].

Apart from the usual SM Feynman rules, the remaining ones necessary for our calculation can be obtained from the above Lagrangians and are presented in Fig. 1. A complete set of Feynman rules for all the $SU(3)_c \times SU(2)_L \times U(1)_Y$ gauge invariant scalar LQ representations are presented in Ref. [171].

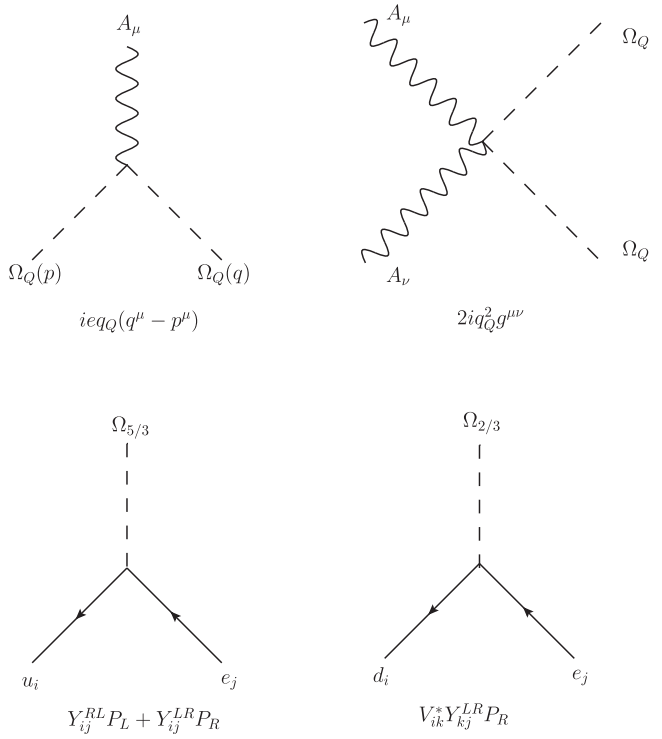

FIG. 1. Feynman rules for the R_2 scalar LQ interactions to the fermions and photon necessary for the calculation of the $f_i \to f_j\gamma\gamma$ decay. All the four-momenta are incoming. The usual SM Feynman rules and also that of the propagator of a scalar particle are not included.

Below we present the calculations of the three-body decay $t \to c\gamma\gamma$.

III. ONE-LOOP SCALAR LQ CONTRIBUTION TO THE $t \to c\gamma\gamma$ DECAY

For the sake of completeness we have obtained general results for the contribution of a scalar LQ with charge Q_S to the decay $f_i \to f_j\gamma\gamma$, where $f_i(f_j)$ can be a lepton or quark. These expressions are useful to calculate both the FCNC top quark decay $t \to c\gamma\gamma$ and the LFV decay $\ell_i \to \ell_j\gamma\gamma$ as well. It is worth noting that our results are also valid for the contribution of other scalar LQs, such as the weak $SU(2)$ singlet $\chi_{1/3}$. Although the interaction of such a scalar LQ to a fermion pair involves Majorana-type Feynman rules that require special treatment, unlike the ones corresponding to the LQ $\Omega_{5/3}$ and $\Omega_{2/3}$ interactions, it can be shown that after some algebra the $\chi_{1/3}$ contributions turn out to be identical to those of $\Omega_{5/3}$ and can be obtained from the latter after replacing the electric charge $Q_{5/3} \to Q_{1/3}$ and the respective coupling constants to fermion pairs. A similar situation arises in the calculation of the LQ contribution to the two-body decay $f_i \to f_j\gamma$, where the results for $\chi_{1/3}$ can be obtained from the contribution of $\Omega_{5/3}$ once the corresponding electric charge and coupling constants are replaced.

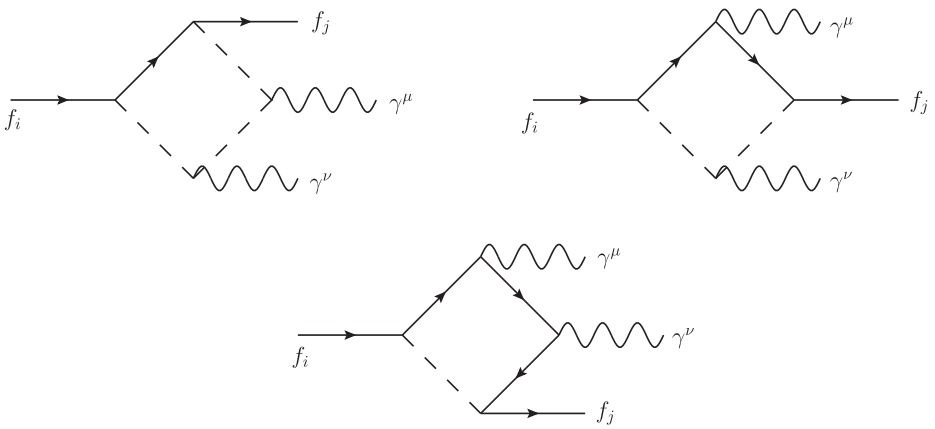

FIG. 2. Box diagrams that contribute to the decay $f_i \to f_j\gamma\gamma$ in the LQ model. There are three additional diagrams that are obtained by exchanging the photons.

For our calculation we use the following convention for the particle four-momenta

$$f_i(p) \to f_j(p')\gamma_\mu(p_1)\gamma_\nu(p_2), \tag{8}$$

with μ and ν the Lorentz indices of the photon four-momenta p_1 and p_2. Hence, the mass-shell conditions are given by $p_1^2 = p_2^2 = 0$, $p^2 = m_i^2$, and $p'^2 = m_j^2$. However we will use the $m_j \to 0$ limit as a good approximation since in all $f_i \to f_j\gamma\gamma$ decays of phenomenological interest the mass of the outgoing fermion is always negligible as compared with the mass of the ingoing fermion. Also, due to the transversality conditions of the photon fields, i.e., $p_1^\mu \epsilon_\mu(p_1) = p_2^\nu \epsilon_\nu(p_2) = 0$, any terms proportional to p_1^μ and p_2^ν can be dropped from the invariant amplitude before contracting with the respective photon polarization vectors. By the same reason, the replacement $p^\nu \to p_1^\nu + p'^\nu$ can also be done throughout the calculation. At the one-loop level, the contribution from $\Omega_{5/3}$ to the rare three-body decay $f_i \to f_j\gamma\gamma$ arises from the box diagrams shown in Fig. 2 as well as the bubble and triangle diagrams of Fig. 3.

After writing out the invariant amplitude for each Feynman diagram, the loop integrals were worked out with the Passarino-Veltman decomposition method [172]. This task was performed with the aid of the *Mathematica* package FeynCalc [173,174], and a cross-check was done via Package-X [175]. We verified that the amplitude is free of ultraviolet divergences and obeys both Bose symmetry and gauge invariance under the $U(1)_{\rm em}$ group. It is worth mentioning that ultraviolet divergences cancel out separately in the amplitude of each set of Feynman diagrams of Figs. 2 and 3, whereas gauge invariance is only achieved after adding up all of the amplitudes.

In the $m_j \to 0$ limit, the invariant amplitude for the decay $f_i \to f_j\gamma\gamma$ can be conveniently written in the following way:

$$\mathcal{M} = \epsilon_\mu^*(p_1)\epsilon_\nu^*(p_2)T^{\alpha\mu}(p_1)T^{\beta\nu}(p_2) \times \bar{f}_j(\mathcal{M}_{L\alpha\beta}P_L + \mathcal{M}_{R\alpha\beta}P_R)f_i, \tag{9}$$

where the tensor $T^{\alpha\beta}(p_i)$ is given by

$$T^{\alpha\beta}(p_i) = \frac{1}{m_i^2}((p_i \cdot p')g^{\alpha\beta} - p_i^\alpha p'^\beta), \tag{10}$$

which clearly obeys

$$T^{\alpha\mu}(p_1)p_{1\mu} = T^{\alpha\nu}(p_2)p_{2\nu} = 0, \tag{11}$$

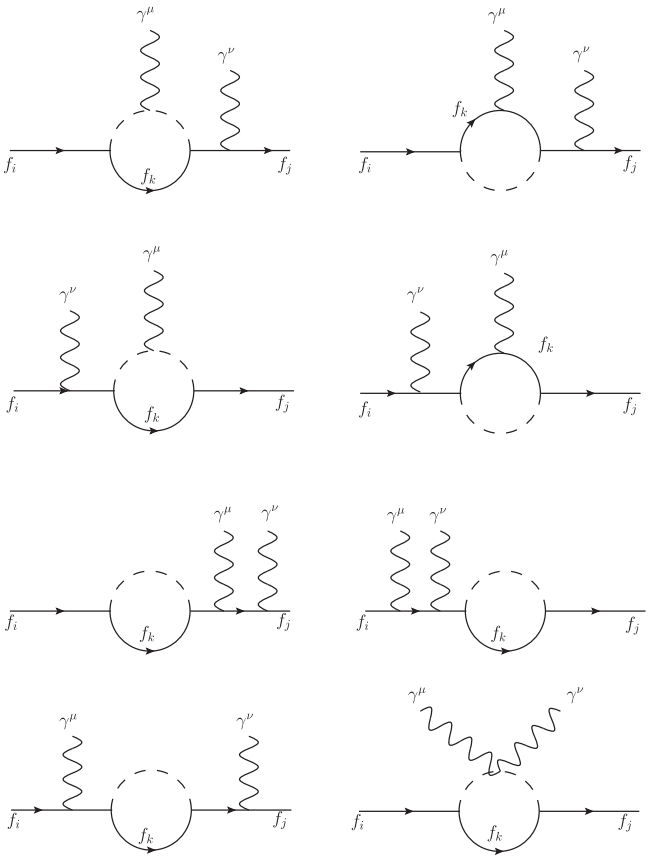

FIG. 3. Bubble and triangle Feynman diagrams for the decay $f_i \to f_j\gamma\gamma$ in the LQ model, where f_i and f_j are quarks (charged leptons) and f_i is a lepton (quark). The crossed diagrams that are obtained by exchanging the photons are not shown.

and thus electromagnetic gauge invariance is manifest. As far as $\mathcal{M}_{L\alpha\beta}$ and $\mathcal{M}_{R\alpha\beta}$ are concerned, they are given in terms of six independent form factors $F_n(\hat{s},\hat{t})$,

$$\mathcal{M}_{L\alpha\beta} = \frac{\alpha N_c}{4\pi m_i}\left[F_1(\hat{s},\hat{t})\gamma_\alpha\gamma_\beta + \frac{1}{m_i}F_2(\hat{s},\hat{t})\gamma_\alpha p_{1\beta} + \frac{1}{m_i^2}F_3(\hat{s},\hat{t})p_{2\alpha}p_{1\beta} + \frac{1}{m_i}\left(F_4(\hat{s},\hat{t})\gamma_\alpha\gamma_\beta + \frac{1}{m_i}F_5(\hat{s},\hat{t})\gamma_\alpha p_{1\beta} + \frac{1}{m_i^2}F_6(\hat{s},\hat{t})p_{2\alpha}p_{1\beta}\right)(\not{p}_1 - \not{p}_2)\right] + \begin{pmatrix} p_{1\mu} \leftrightarrow p_{2\nu} \\ \hat{s} \leftrightarrow \hat{t} \end{pmatrix}, \tag{12}$$

where we introduced the Mandelstam-like scaled variables

$$\hat{s} = \frac{1}{m_i^2}(p - p_1)^2,$$
$$\hat{t} = \frac{1}{m_i^2}(p - p_2)^2.$$

A similar expression to Eq. (12) holds for $\mathcal{M}_{R\alpha\beta}$ but with F_n replaced by $\tilde{F}_n$ ($n = 1, \ldots 6$), which is obtained from F_n as follows:

$$\tilde{F}_n = F_n\begin{pmatrix} Y_{ik}^{RL} \leftrightarrow Y_{ik}^{LR} \\ Y_{jk}^{RL} \leftrightarrow Y_{jk}^{LR} \end{pmatrix}. \tag{13}$$

From the above expressions, it is easy to show that Bose symmetry is obeyed.

The contributions of our LQ model to the $F_n(\hat{s},\hat{t})$ form factors are presented in Appendix A in terms of Passarino-Veltman integral coefficients. The decay width is given by

$$\Gamma(f_i \to f_j\gamma\gamma) = \frac{m_i}{256\pi^3}\int_0^1 d\hat{s}\int_0^{1-\hat{s}} d\hat{t}|\bar{\mathcal{M}}|^2, \tag{14}$$

where the average square amplitude is presented for completeness in Appendix B.

From our general expressions for the decay $f_i \to f_j\gamma\gamma$, we can easily obtain the invariant amplitude and decay width of the $t \to c\gamma\gamma$ process, in which case the internal fermion f_k in the Feynman diagrams of Figs. 2 and 3 is a charged lepton. We thus set the mass of the decaying and internal fermions as $m_i \to m_t$ and $m_k = m_\ell$ with $\ell = \mu, \tau$, whereas for the final fermion we use $m_c \simeq 0$.

IV. LQ PARAMETER SPACE CONSTRAINTS

We now discuss the constraints from experimental data on the parameter space of the model and examine two scenarios: one with a single LQ doublet and another with multiple LQ doublets. Below we will concentrate on the bounds on the LQ masses and the couplings constants $Y_{i\ell_j}^{RL,LR}$, which are required to obtain an estimate for the decay $t \to c\gamma\gamma$.

A. Bounds on LQ mass

The most up-to-date constraints on the masses of various kinds of vector and scalar LQs have been obtained from the data of direct searches for LQs at the LHC by the CMS and ATLAS collaborations. Scalar LQs have been searched for through single production $pp \to S\bar{\ell} \to q\ell\bar{\ell}$ or pair production $pp \to S^\dagger S \to q\bar{q}\ell\bar{\ell}, q\bar{q}\nu\bar{\nu}$, thereby yielding bounds on the LQ masses, which depend on the LQ decay channels and the size of their couplings to fermions. Most of these bounds rely on the assumption that LQs can only couple to one generation of fermions and have a dominant decay channel, though very recently a more general scenario where LQs can couple simultaneously to fermions of distinct generations was analyzed [167,168,176]. Since a scalar LQ doublet with nondegenerate mass components can give dangerous contributions to the oblique parameters, we consider that both components of the scalar LQ doublet R_2 are mass degenerate, which indeed is true at the lowest order in v. We thus need to consider the current bounds on the masses of LQs of electric charges $2/3$ and $5/3$.

For the mass of a charge $5/3$ LQ, the most stringent bound was obtained by the CMS collaboration [177] by using data collected in 2016 at $\sqrt{s} = 13$ TeV and assuming that the main LQ decay mode is that into a top quark and a tau lepton. Such an analysis has excluded a charge $5/3e$ scalar LQ with a mass below 900 GeV. As for the bounds on other types of scalar LQs, they are more stringent, slightly above 1 TeV. For instance, for the mass of a third-generation charge $2/3e$ scalar LQ decaying into $b\tau/t\nu_\tau$, the ATLAS collaboration [178] has set a lower bound of about 1.2 TeV. As already mentioned, such a charge $2/3$ scalar LQ can be identified with the second component of the R_2 doublet, and thus the mass constraint would apply to both $\Omega_{2/3}$ and $\Omega_{5/3}$ if they are considered mass degenerate.

There are also theoretical analyses where the parameter space of scalar LQs has been constrained via the LHC data [179]. If one considers models where LQs provide an explanation for the LFUV anomalies in B meson decays, LQ couplings slightly larger than $O(1)$ are required. In this scenario, more stringent constraints on the LQ masses arise from LQ pair production [50,53], ranging from 1 to 2 TeV.

In our analysis below we consider LQ masses above 1 TeV and impose constraints on the LQ couplings to fermions such that no dangerous LQ-mediated contributions to observable quantities are induced.

B. Bounds on LQ couplings

In order to discuss the constraints on the LQ couplings we will consider the following two scenarios, which can allow us to asses the order of magnitude of the $t \to c\gamma\gamma$ branching ratio.

Scenario I. There is only one LQ doublet R_2 that has both left- and right-handed couplings to fermions of the second and third generations only, namely, $Y_{i\ell}^{RL,LR}$, where $\ell = \mu, \tau$ and $i = 2, 3$ stands for the quark generation. In this scenario there are LFV transitions between the muon and the tau lepton, and there is indeed an explanation for the muon $g-2$ anomaly, though an explanation for the apparent LFUV anomalies in B meson decays is not favored. This model was considered in our previous work on the two-body top quark decays $t \to cX$ ($X = \gamma$, g, H, Z) [22], and constraints on the parameter space were obtained from the muon $g-2$ anomaly and the LFV decay $\tau \to \mu\gamma$, together with extra constraints to avoid large contributions to other observable quantities.

Scenario II. There are multiple LQ doublets R_2. As an example of this realization we will consider the model recently proposed in [154], where the SM is augmented with one LQ doublet R_2^ℓ ($\ell = e, \mu, \tau$) for each lepton generation. Although each LQ doublet can only couple to the leptons of one generation, thereby forbidding LFV, all of them can couple to the quarks of the second and third generations. This scenario provides an explanation for the a_μ anomaly and the LFUV anomalies in B meson decays, which requires relatively large LQ couplings, though as mentioned above recent data seems to exclude the R_K and R_{K^*} anomalies. An analysis on the constraints on the parameter space of this model was presented in Ref. [154].

Below we analyze the constraints on the LQ couplings in the above scenarios and focus on the allowed parameter space region most promising for the $t \to c\gamma\gamma$ branching ratio.

1. Scenario I

In our analysis we will follow our previous work [22], where we assumed that the $\Omega_{5/3}$ scalar LQ is responsible for the muon $g-2$ anomaly and considered the bounds on the $Y_{i\mu}^{LR,RL}$ and $Y_{i\tau}^{LR,RL}$ couplings obtained from the LFV decay $\tau \to \mu\gamma$. The analytical expressions for the contribution of a scalar LQ to the muon anomalous magnetic dipole moment (AMDM) and the LFV decay $\ell_i \to \ell_j\gamma$ were obtained long ago and were also reproduced in Ref. [22,135] in terms of Feynman parameter integrals and Passarino-Veltman scalar functions. For the sake of completeness we present such results in Appendix C. Note that a_μ contains a chirality flipping term proportional to $m_{q_i} \times \mathrm{Re}(Y_{i\mu}^{RL} Y_{i\mu}^{LR*})$, which gives the dominant contribution for a heavy internal quark. Since such contribution requires that the scalar LQ has both left- and right-handed couplings to the fermions, it is absent for chiral LQs. Thus the contribution to a_μ from the chiral LQ $\Omega_{2/3}$ via an internal b quark is expected to be much smaller than the contribution from the nonchiral LQ $\Omega_{5/3}$.

As far as the experimental constraints are concerned, for the muon AMDM a_μ we consider the current average of its experimental measurements [180,181], whereas for the SM theoretical prediction we consider the estimate obtained by the muon $g-2$ theory initiative [182]. This yields the following 4.2σ discrepancy between theory and experiment:

$$\Delta a_\mu = 251(59) \times 10^{-11}. \tag{15}$$

For the decay $\tau \to \mu\gamma$, the expected future experimental sensitivity [183] puts strong constraints on LFV processes between the second and third generations

$$\mathrm{Br}(\tau \to \mu\gamma) \leq 1.0 \times 10^{-9}, \tag{16}$$

but we will consider the current experimental constraint [184]

$$\mathrm{Br}(\tau \to \mu\gamma) \leq 4.4 \times 10^{-8}. \tag{17}$$

Note that $\Omega_{5/3}$ and $\Omega_{2/3}$ can also give dangerous contributions to several observable quantities through their couplings to the $\bar{b}\tau$ and $t\nu_\tau$ pairs both at the tree and one-loop level. Therefore one must verify that the values of the LQ couplings consistent with the muon $g-2$ discrepancy and the constraint on the $\tau \to \mu\gamma$ decay do not introduce tension between the theory predictions and experimental data. For instance at the LHC, double (single) tau lepton production $\tau^-\tau^+$ ($\tau\nu$) can arise at the tree level via single LQ production $pp \to S\ell^+ \to q\ell^-\ell^+$ ($pp \to S\ell^+ \to q\nu\ell^+$), with q being identified with a single jet. On the other hand, among those observable quantities sensitive to large LQ couplings at the one-loop level there are the decays $Z \to \tau^-\tau^+$ and $Z \to \nu\nu$. We will thus impose the additional constraints $|Y_{i\mu}^{LR,RL}| < 1$, which ensures that no tension will arise between the theory predictions and the experimental data [53,154]. This is a more stringent constraint than $|Y_{i\mu}^{LR,RL}| < 4\pi$, which is usually imposed to avoid the breakdown of perturbation theory.

Rather than making any *a priori* assumption about the LQ coupling constants to leptons and quarks, we consider nonvanishing left- and right-handed couplings to the leptons and quarks of both the second and third

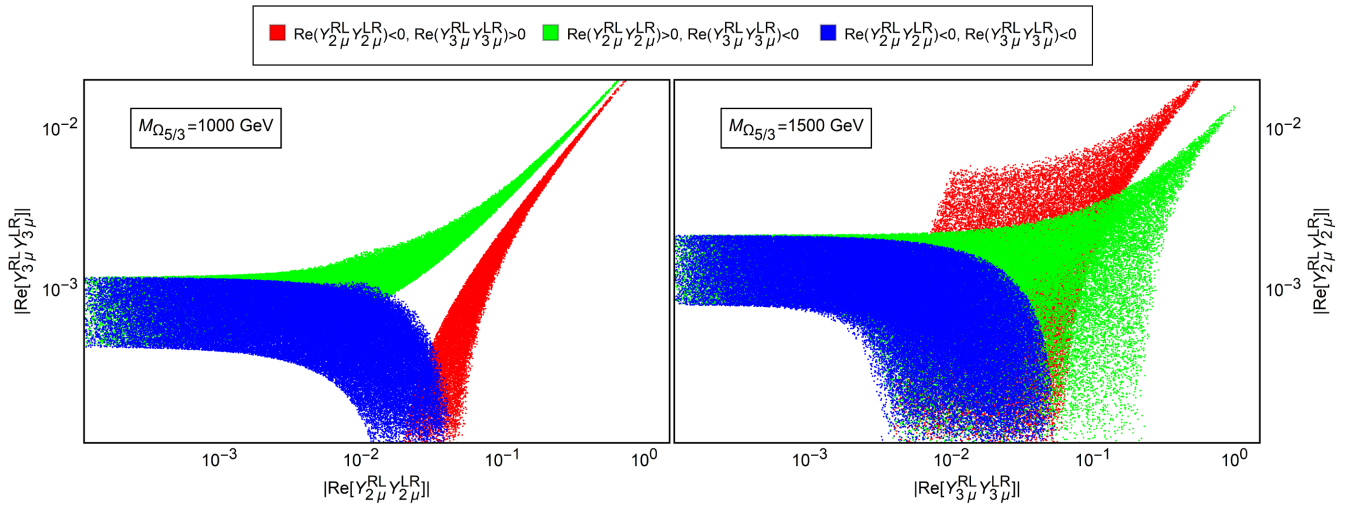

FIG. 4. Allowed area on the $\mathrm{Re}(Y^{RL}_{2\mu}Y^{LR}_{2\mu})$ vs $\mathrm{Re}(Y^{RL}_{3\mu}Y^{LR}_{3\mu})$ plane consistent with the muon $g-2$ anomaly at 95% C.L. for a charge 5/3 scalar LQ with mass of 1 and 1.5 TeV in three scenarios of the signs of the $\mathrm{Re}(Y^{RL}_{i\mu}Y^{LR}_{i\mu})$ products, which determine the signs of the partial contributions. As explained in the text, we also impose the extra constraints $|Y^{LR,RL}_{i\mu}|<1$ to be consistent with other constraints from experimental data.

generations: $Y^{LR,RL}_{i\mu}$, where i stands for the generation quark. Without losing generality we consider purely real LQ couplings and randomly scan for a few thousands of 4-tuples $\{Y^{RL}_{2\mu}, Y^{LR}_{2\mu}, Y^{RL}_{3\mu}, Y^{LR}_{3\mu}\}$ consistent with the discrepancy of the muon $g-2$ anomaly at 95% C.L. The allowed region is shown in Fig. 4 on the $\mathrm{Re}(Y^{RL}_{2\mu}Y^{LR}_{2\mu})$ vs $\mathrm{Re}(Y^{RL}_{3\mu}Y^{LR}_{3\mu})$ plane for a charge 5/3 scalar LQ with a mass of 1 and 1.5 TeV.

In our analysis we have considered three scenarios for the relative signs of the products of the left- and right-handed couplings $\mathrm{Re}(Y^{RL}_{i\mu}Y^{LR}_{i\mu})$ as they determine the sign of the contribution to a_μ from the quark of generation i. We observe that the largest values for the coupling products are allowed when they have opposite signs (red and green points) as large partial contributions can cancel each other out to give the required negative total contribution. On the other hand, in the scenario when both couplings are negative (blue points), the partial contributions add up, thereby imposing a tighter constraint of the LQ coupling products.

Unless an additional flavor symmetry is introduced, $\Omega_{5/3}$ can also couple to the τ lepton and induce LFV processes. Thus the decay $\tau\to\mu\gamma$ imposes an extra constraint on the $Y^{RL,LR}_{i\mu}$ and $Y^{RL,LR}_{i\tau}$ couplings, which must be combined with that arising from the muon $g-2$ anomaly. Again we do not impose an *a priori* condition for the coupling constants and randomly scan for a set of points $\{Y^{RL}_{2\ell}, Y^{LR}_{2\ell}, Y^{RL}_{3\ell}, Y^{LR}_{3\ell}\}$ ($\ell=\mu,\tau$) consistent with the discrepancy of the muon $g-2$ anomaly and the experimental upper bound on the $\tau\to\mu\gamma$ decay, along with the extra upper bounds $|Y^{RL,LR}_{i\ell}|\leq 1$. It turns out that the $t\to c\gamma\gamma$ invariant amplitude of Eq. (9) is given in terms of form factors of the form (see Appendix A)

$$F_n=\sum_{\ell_k=\mu,\tau}(f^{LL}_n Y^{RL}_{i\ell_k}Y^{RL}_{j\ell_k}+f^{RR}_n Y^{LR}_{i\ell_k}Y^{LR}_{j\ell_k}+f^{RL}_n Y^{LR}_{i\ell_k}Y^{RL}_{j\ell_k}+f^{LR}_n Y^{RL}_{i\ell_k}Y^{LR}_{j\ell_k}). \tag{18}$$

From our numerical analysis of the allowed values for the LQ coupling constants, we infer that from all the products of coupling constants of Eq. (18), the ones that can reach the largest allowed values are $Y^{RL}_{3\mu}Y^{RL}_{2\mu}$ and $Y^{LR}_{3\tau}Y^{LR}_{2\tau}$, whereas the remaining products are much more constrained. Therefore the $t\to c\gamma\gamma$ decay width will depend mainly on the values of this pair of coupling products and would reach its maximal value when one of them reaches its largest allowed values. We thus show the allowed region on the $\mathrm{Re}(Y^{RL}_{2\tau}Y^{RL}_{3\tau})$ vs $\mathrm{Re}(Y^{LR}_{2\tau}Y^{LR}_{3\tau})$ plane in Fig. 5 and on the $\mathrm{Re}(Y^{RL}_{2\mu}Y^{RL}_{3\mu})$ vs $\mathrm{Re}(Y^{LR}_{2\mu}Y^{LR}_{3\mu})$ plane in Fig. 6 for a scalar LQ $\Omega_{5/3}$ with mass of 1 TeV (top plots) and 1.5 TeV (bottom plots) in the three scenarios of the signs of the products $\mathrm{Re}(Y^{RL}_{i\mu}Y^{LR}_{i\mu})$ of Fig. 4.

We can conclude that the largest allowed values correspond to $Y^{LR}_{2\tau}Y^{LR}_{3\tau}$ products, which are obtained when both the c and t contributions to a_μ have opposite signs (red and green points). The products of LQ couplings to the muon are more restricted, which is due to the condition imposed by the muon $g-2$ anomaly. For illustration purposes, in Table I we show a few sets of values in which the product $Y^{LR}_{2\tau}Y^{LR}_{3\tau}$ reaches its largest allowed values, which are slightly below the unity. These sets of points would yield

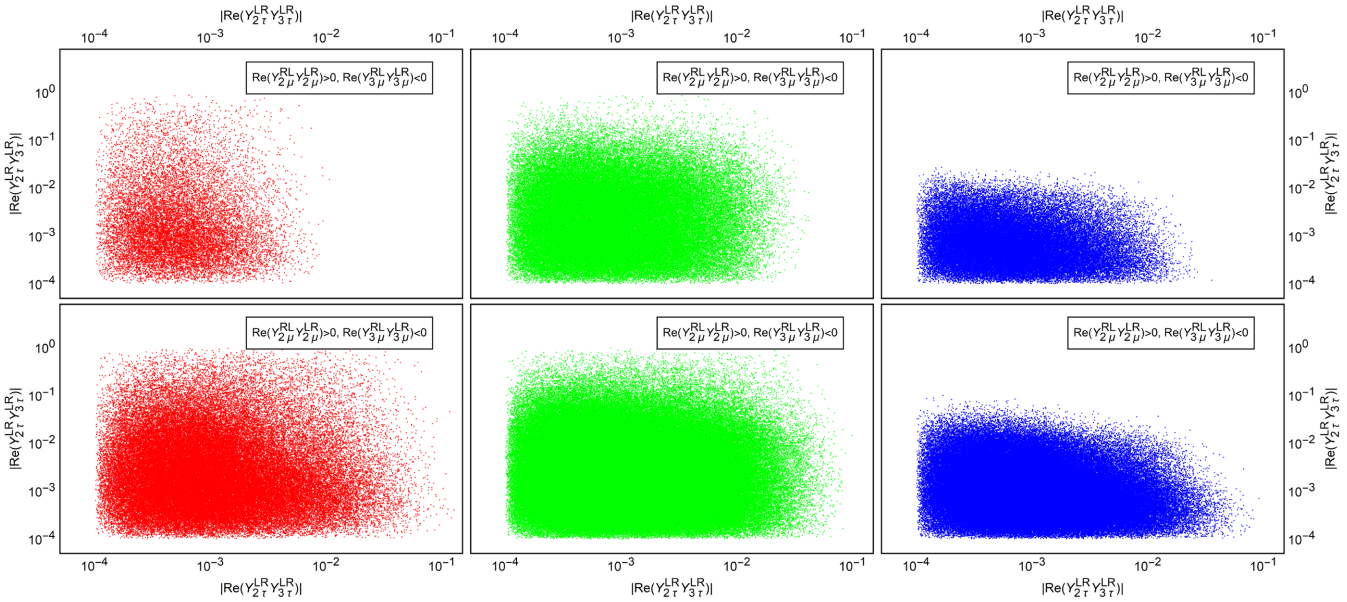

FIG. 5. Allowed area on the $\mathrm{Re}(Y^{RL}_{2\tau}Y^{RL}_{3\tau})$ vs $\mathrm{Re}(Y^{LR}_{2\tau}Y^{LR}_{3\tau})$ plane consistent with the muon $g-2$ anomaly at 95% C.L. and the LFV decay $\tau \to \mu\gamma$ for a scalar LQ $\Omega_{5/3}$ with mass of 1 TeV (top plots) and 1.5 TeV (bottom plots) in the three scenarios of the signs of the products $\mathrm{Re}(Y^{RL}_{i\mu}Y^{LR}_{i\mu})$ considered in Fig 4. The constraint $|Y^{RL,LR}_{i\ell}| \leq 1$ is also imposed to be consistent with other experimental constraints.

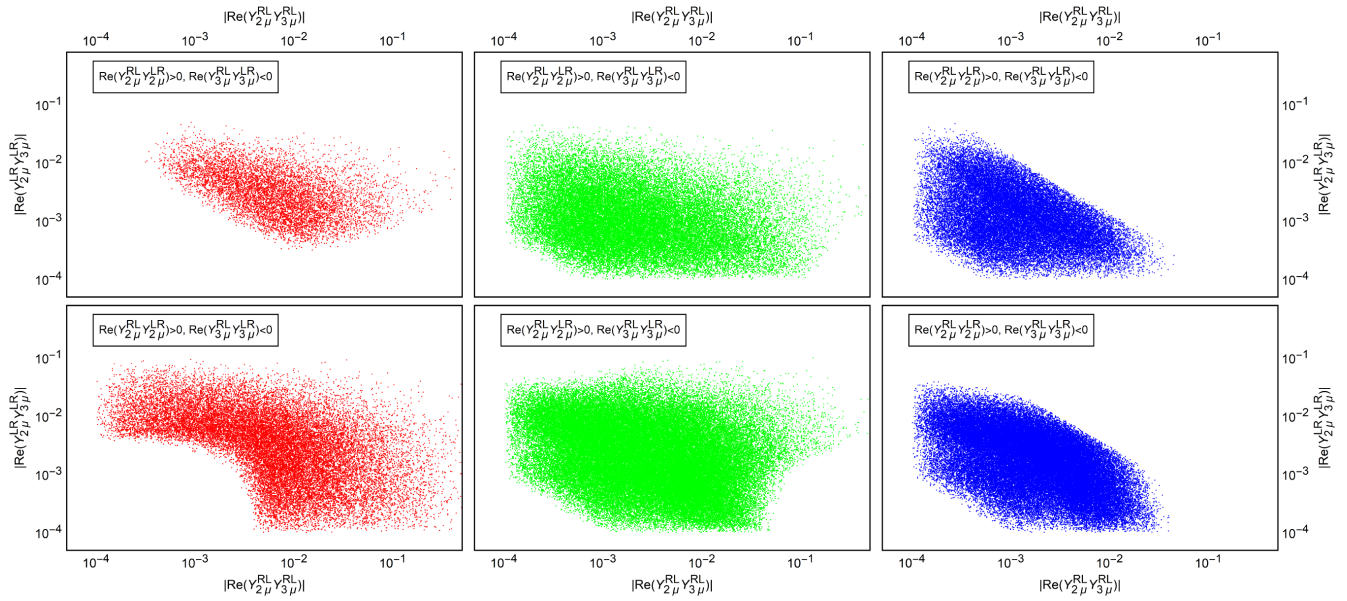

FIG. 6. The same as in Fig. 5 but for the allowed area on the $\mathrm{Re}(Y^{RL}_{2\mu}Y^{RL}_{3\mu})$ vs $\mathrm{Re}(Y^{LR}_{2\mu}Y^{LR}_{3\mu})$ plane.

the maximal values of the $t \to c\gamma\gamma$ branching ratio in scenario I.

Also, as expected we observe that the constraints on the LQ couplings are relaxed when the LQ mass increases and the allowed area enlarges slightly when the LQ increases from 1 to 1.5 TeV. However, although the LQ couplings could be less restricted, a possible enhancement of the $t \to c\gamma\gamma$ branching ratio may be suppressed by the larger value of the LQ mass.

2. Scenario II

Motivated by the apparent anomalies in B meson decays, quite recently the authors of Ref. [154] introduced a model

TABLE I. Sample sets of values of LQ couplings to fermions consistent with the muon $g-2$ anomaly and the experimental constraint on the LFV decay $\tau \to \mu\gamma$ for $m_{R_2} = 1$ TeV (rows 1 through 3) and $m_{R_2} = 1.5$ TeV (rows 4 through 7) in scenario I. The last row shows the allowed values consistent with an explanation for the R_D and R_{D^*} anomalies, the muon $g-2$ discrepancy, and other experimental constraints for $m_{R_2^\mu} = 1.7$ TeV and $m_{R_2^\mu} = 2$ TeV in scenario II (see [154]), which also explains the apparent R_K and R_{K^*} anomalies, which seem to be excluded by recent data [157]. Results taken from Ref. [154].

Scenario	LQ mass (TeV)	$Y^{RL}_{2\mu}$	$Y^{LR}_{2\mu}$	$Y^{RL}_{3\mu}$	$Y^{LR}_{3\mu}$	$Y^{RL}_{2\tau}$	$Y^{LR}_{2\tau}$	$Y^{RL}_{3\tau}$	$Y^{LR}_{3\tau}$
I	1.0	−0.167	0.246	0.011	0.018	0.059	0.92	0.015	0.88
I	1.0	0.949	0.013	−0.073	0.018	0.011	0.917	0.018	0.798
I	1.0	0.193	0.019	−0.014	0.044	0.024	0.978	0.012	0.888
I	1.5	0.431	0.041	−0.025	0.011	0.037	0.994	0.016	0.831
I	1.5	0.424	0.012	−0.02	0.021	0.023	0.957	0.041	0.917
I	1.5	−0.236	0.155	0.012	0.038	0.016	0.958	0.013	0.995
II	1.7 (R^τ), 2.0 (R^μ)	⋯	⋯	2.4–2.6	-7×10^{-3}	2.4–2.55	0.3–0.35	⋯	0.9–1.1

with one LQ doublet R_2^ℓ ($\ell = \mu,\ \tau$) for each lepton generation. In order to avoid dangerous LFV effects induced by large LQ couplings, required by the LFUV B meson anomalies, an additional flavor symmetry was imposed so that each scalar LQ doublet can only couple to one lepton generation, though they still have couplings to quarks of the second and third generations. Therefore, although no LQ-mediated LFV processes arise, FCNC top quark decays could still be allowed at the one-loop level.

A comprehensive analysis of the bounds on LQ R_2^τ couplings obtained from several observable quantities was presented in Ref. [154]. It was shown that one scalar LQ doublet R_2^τ with a mass of 1.7 TeV can explain the R_D and R_{D^*} anomalies, provided that the values of the coupling constants $Y^{LR}_{3\tau}$ and $Y^{RL*}_{2\tau}$ are slightly larger than $O(1)$ and there is a large complex phase in the product of both coupling constants. This is still consistent with the data on $\tau\nu$ and $\tau^-\tau^+$ production at the LHC, but some tension could arise in the electroweak fit for the data of the decays $Z \to \tau^-\tau^+$ and $Z \to \bar{\nu}\nu$ [154]. Also, the constraint $Y^{LR}_{2\tau}Y^{LR*}_{3\tau} \lesssim 0.25$ is obtained from $B_s - \bar{B}_s^*$ mixing [154].

The R_2^τ doublet alone gives no explanation for both the muon $g-2$ discrepancy and the apparent R_K and R_{K^*} anomalies, for which a second doublet LQ doublet R_2^μ is necessary [154]. It was shown that the presence of two scalar doublets improves the fit of the $b \to s\ell^-\ell^+$ data and relaxes the tension in the electroweak data as smaller R_2^τ couplings are required to explain the R_D and R_{D^*} anomalies for $M_{R_2^\mu} = 2$ TeV and $M_{R_2^\tau} = 1.7$ TeV. A summary of the values of the coupling constants consistent with the LFUV anomalies in B decays and the a_μ anomaly, taken from Ref. [154], is shown in the last row of Table I. Note that the LQ doublet R_2^τ alone could yield an enhanced branching ratio for FCNC top quark decays due to the large LQ couplings, though an additional suppression due to the heavier value of the LQ mass is expected too.

Following the notation of Ref. [50] we present in Table II the main features of the scenarios just discussed. It seems that scenario II is the most promising for a less suppressed $t \to c\gamma\gamma$ branching ratio as LQ couplings to the τ lepton of the order of $O(1)$ are allowed; however, a larger mass is also necessary to fulfill the constraints from experimental data, which may result in an additional suppression. Below we present an estimate for the $t \to c\gamma\gamma$ branching ratio in these scenarios.

C. Estimate of the $t \to c\gamma\gamma$ branching ratio

For the numerical evaluation of the invariant amplitude (9) and to achieve a best numerical stability in the evaluation of the double integral of Eq. (14), we decomposed the Passarino-Veltman integrals of Eqs. (A4) through (A44) into scalar functions (the results are too lengthy to be presented in this work), which then were evaluated through the LoopTools [185,186] package. Also, an independent evaluation was performed via the Collier package [187], which showed a good agreement with the LoopTools evaluation. To obtain the $t \to c\gamma\gamma$ decay width we impose the kinematic cuts $E_\gamma > 5$ GeV for both photons.

As far as scenario I is concerned, from the above analysis we can conclude that the contribution to the $t \to c\gamma\gamma$ decay width from the loops with an internal muon is much smaller than that from the loops with an internal tau lepton, which is due to the small allowed values of the LQ-muon couplings. In fact we can neglect the muon contribution to the $t \to c\gamma\gamma$ invariant amplitude as it is more than 2 orders of magnitude below the one of the tau lepton.

TABLE II. Scenarios discussed in the text along with the anomalies addressed and other predicted new physics effects. Note that the R_{K^*} anomaly seems to be excluded by the recent LHCb measurement [157].

Scenario	a_μ	R_D, R_{D^*}	R_{K^*}	LFV	FCNC
I	✓	✗	✗	✓	✓
II with R_2^τ alone	✗	✓	✗	✗	✓
II with both R_2^μ and R_2^τ	✓	✓	✓	✗	✓

Therefore, the largest values of the $t \to c\gamma\gamma$ decay width for a specific value of the LQ mass are reached in the region where the product of couplings $Y_{2\tau}^{LR} Y_{3\tau}^{LR}$ reaches its largest allowed values. In this region the behavior of the $t \to c\gamma\gamma$ branching ratio as a function of the LQ coupling can be roughly approximated as

$$\mathrm{Br}(t \to c\gamma\gamma) \simeq f(m_S, m_c, m_t, m_\tau)|Y_{2\tau}^{LR} Y_{3\tau}^{LR}|^2, \quad (19)$$

with $f(m_S, m_c, m_t, m_\tau)$ of the order of $10^{-11} - 10^{-10}$ at most for $m_S \simeq 1$ TeV .

In Fig. 7 we show the behavior of the LQ contribution to $\mathrm{Br}(t \to c\gamma\gamma)$ in scenario I as a function of the LQ mass around the region where the $Y_{2\tau}^{LR} Y_{3\tau}^{LR}$ product reaches its largest allowed values and thus $\mathrm{Br}(t \to c\gamma\gamma)$ reaches its largest values. For illustration purposes we also show the case where the product $Y_{2\tau}^{RL} Y_{3\tau}^{RL}$ would dominate over $Y_{2\tau}^{LR} Y_{3\tau}^{LR}$, though in this case $\mathrm{Br}(t \to c\gamma\gamma)$ does not reach its largest values as $Y_{2\tau}^{RL} Y_{3\tau}^{RL}$ is allowed to be of the order of 10^{-1} at most.

We can conclude that the LQ contribution to $\mathrm{Br}(t \to c\gamma\gamma)$ can be of the order of 10^{-11} at most for $Y_{2\tau}^{LR} Y_{3\tau}^{LR}$ of the order of $O(1)$, though it would decrease considerably if the LQ couplings decrease by 1 order of magnitude. Also, we note that there is little dependence on the LQ mass in the interval from 1 to 2 TeV.

As for scenario II, according to the allowed values of the LQ couplings presented in Table I from Ref. [154], $\mathrm{Br}(t \to c\gamma\gamma)$ would be dominated by the R_2^τ contribution since any products of R_2^μ couplings that enter into Eq. (18) would be considerably suppressed. Furthermore, the dominant term arises from the $Y_{2\tau}^{RL} Y_{3\tau}^{LR}$ product. In this case we obtain for $m_{R_2^\tau} = 1.7$ TeV

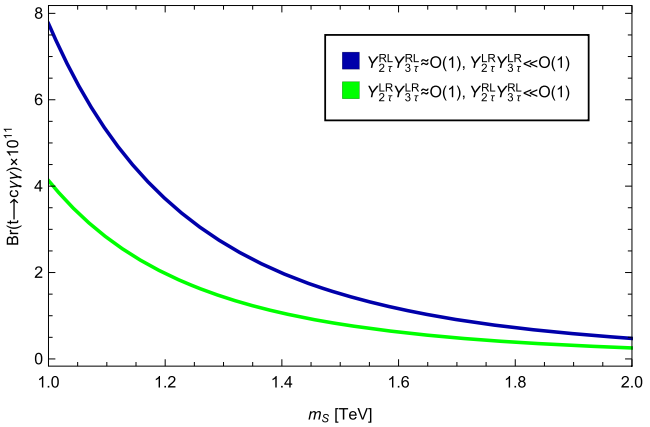

FIG. 7. LQ contribution to the branching ratio of the $t \to c\gamma\gamma$ decay in scenario I as a function of the LQ mass in the region of the parameter space where the product $Y_{2\tau}^{LR} Y_{3\tau}^{LR} \sim O(1)$ reaches its largest allowed values, which corresponds to the largest possible value of $\mathrm{Br}(t \to c\gamma\gamma)$. We also include the case where the product $Y_{2\tau}^{RL} Y_{3\tau}^{RL}$ dominates over $Y_{2\tau}^{LR} Y_{3\tau}^{LR}$ for $Y_{2\tau}^{RL} Y_{3\tau}^{RL} \simeq O(1)$, though this is not allowed by the constraints from experimental data.

TABLE III. Largest estimated values of the one-loop contributions to two- and three-body FCNC top quark decays from models with scalar $SU(2)$ doublets consistent with the current constraints from experimental data [22].

Decay channel	Branching ratio $m_{R_2} = 1$ TeV	Branching ratio $m_{R_2} = 1.5$ TeV
$t \to c\gamma$	10^{-9}	10^{-9}
$t \to cg$	10^{-9}	10^{-10}
$t \to cZ$	10^{-8}	10^{-9}
$t \to cH$	10^{-9}	10^{-10}
$t \to c\mu^-\mu^+$	10^{-6}	10^{-7}
$t \to c\tau^-\tau^+$	10^{-7}	10^{-8}
$t \to c\gamma\gamma$	10^{-11}	10^{-12}

$$\mathrm{Br}(t \to c\gamma\gamma) \simeq 9.11 \times 10^{-12} \times |Y_{2\tau}^{RL} Y_{3\tau}^{LR}|^2, \quad (20)$$

where we have neglected all other contributions. For $Y_{2\tau}^{RL} \simeq 2$ and $Y_{3\tau}^{LR} \simeq 1$ we obtain again the estimate $\mathrm{Br}(t \to c\gamma\gamma) \simeq 10^{-11}$. Therefore, in both scenarios I and II, the $t \to c\gamma\gamma$ branching ratio would reach values as high as $10^{-12} - 10^{-11}$. These are the largest possible values that one can expect for the contribution to the $t \to c\gamma\gamma$ decay from the R_2 doublet scalar LQs since experimental constraints severely constrain the LQ coupling constants. Thus, unless an extraordinary cancellation in the LQ contribution to experimental observable quantities (fine tuning) occurs in a more sophisticated framework with additional LQ multiplets, the LQ contribution to the $t \to c\gamma\gamma$ decay is expected to be beyond the reach of measurement.

In Table III we present a summary of the one-loop contributions to two- and three-body FCNC top quark decays from a scalar $SU(2)$ doublet from Ref. [22] and this work. We have considered the largest estimate consistent with the current constraints from experimental data.

V. FINAL REMARKS

In this work we have presented a calculation of the rare three-body FCNC top quark decay $t \to c\gamma\gamma$ in the framework of a renormalizable model where the SM is augmented with one or three $SU(2)$ scalar LQ doublets with hypercharge $7/6$, which gives rise to two scalar LQs with electric charge of $5/3$ and $2/3$. We considered two particular scenarios: a minimal model with a lone scalar LQ doublet (scenario I) and another model with three scalar LQ doublets R_2^ℓ ($\ell = \mu, \tau$) (scenario II). While scenario I can address the muon $g-2$ anomaly, scenario II was proposed recently [154] to also explain the LFUV anomalies in b-hadron decays. The general aspects and the generic Lagrangian and Feynman rules for this class of models are discussed, and analytical expressions for the one-loop LQ contribution to the invariant amplitude of the general decay $f_i \to f_j\gamma\gamma$ are presented in terms of Passarino-Veltman integral coefficients, from which the corresponding invariant amplitude for the decay $t \to c\gamma\gamma$ follows easily.

A discussion of the current bounds on the LQ masses and the LQ couplings to leptons and quarks is also presented. In scenario I the region of allowed values of LQ couplings is found by requiring that the charge $5/3$ is responsible for the muon $g-2$ discrepancy and obeys the constraint on the LFV decay $\tau \to \mu\gamma$ as well as the extra constraint on the LQ couplings $|Y_{i\ell}^{LR,RL}| \leq 1$, which is imposed to avoid tension with experimental data of processes sensitive to LQ contributions. It is found that the LQ couplings can be as large as 0.1–1 for a LQ mass around 1 TeV, which results in a branching ratio for the $t \to c\gamma\gamma$ decay of the order of 10^{-11}–10^{-12}. When the mass of the LQ increases up to around 1.5 TeV, this branching ratio decreases slowly, but there is a high dependence on the magnitude of the LQ coupling constants.

As far as scenario II is concerned, we consider the bounds obtained in the analysis of Ref. [154], where the parameter space of the model was constrained by requiring a solution to the LFUV anomalies and the muon $g-2$ discrepancy, along with constraints from experimental data. For a LQ doublet R_2^τ with a mass of 1.7 TeV, LQ couplings to the τt pair with values slightly larger than $O(1)$ are still allowed, whereas the couplings of the R_2^μ doublet would be 1 or 2 orders of magnitude below for a LQ mass of 2 TeV. In this scenario the branching ratio of the $t \to c\gamma\gamma$ decay is also of the order of 10^{-11}–10^{-12}.

In conclusion the LQ contribution to the branching ratio of the three-body decay $t \to c\gamma\gamma$ is about 2 or 3 orders of magnitude below the one for the two-body decay $t \to c\gamma$, which is below the expected experimental reach.

The supporting data for this paper are openly available from [188].

ACKNOWLEDGMENTS

The work of R. Sánchez-Vélez was partially supported by Consejo Nacional de Ciencia y Tecnología under Grant No. A1-S-23238. G. Tavares-Velasco acknowledges partial support from Sistema Nacional de Investigadores (Mexico) and Vicerrectoría de Investigación y Estudios de Posgrado de la Benémerita Universidad Autónoma de Puebla.

APPENDIX A: ANALYTICAL RESULTS FOR THE $f_i \to f_j\gamma\gamma$ FORM FACTORS

The form factors F_n $(n = 1\ldots6)$ of Eq. (12) were obtained in terms of Passarino-Veltman scalar functions with the help of the FeynCalc package [173,174], and a cross-check was done via Package-X [175]. Since the results in terms of Passarino-Veltman scalar functions are too lengthy to be shown here, we present our results in terms of the coefficients of two-. three-, and four-point tensor integrals: B_1, B_{ii}, C_i, C_{ij}, etc., where we follow the notation of Ref. [173]. Note however that in order to simplify our results, a scale factor was introduced to obtain dimensionless three- and four-point scalar functions as well as dimensionless tensor integral coefficients: all three-point scalar functions and tensor integral coefficients, but $C_{00}(i)$, are scaled by m_i^{-2}, whereas all four-point scalar functions and tensor integral coefficients, but $D_{00}(i)$ and $D_{00j}(i)$, are scaled by m_i^{-4}.

As already mentioned, we consider the $m_j \simeq 0$ limit (an outgoing massless fermion) and define Mandelstam-like scaled variables $\hat{s} = (p' + p_2)^2/m_i^2 \simeq 2p' \cdot p_2/m_i^2$, $\hat{t} = (p' + p_1)^2 \simeq 2p_1 \cdot p'/m_i^2$, and $\hat{u} = (p_1 + p_2)^2/m_i^2 = 2p_1 \cdot p_2/m_i^2$, which obey $\hat{s} + \hat{t} + \hat{u} = 1$. We also define the auxiliary variables $x_a = m_a^2/m_i^2$, $y_a = m_a/m_i$, for $a = k, S$, where the subscript k stands for the virtual fermion. Furthermore, $\delta_s = \hat{s} - 1$, $\delta_t = \hat{t} - 1$, and the electric charges of the external fermions Q_i and the internal one Q_k are given in units of e.

The form factors F_n $(n = 1, \ldots, 6)$ of Eq. (12) can be written as

$$F_n = \sum_{\ell_k=\mu,\tau} (f_n^{LL} Y_{i\ell_k}^{RL} Y_{j\ell_k}^{RL} + f_n^{RR} Y_{i\ell_k}^{LR} Y_{j\ell_k}^{LR} + f_n^{RL} Y_{i\ell_k}^{LR} Y_{j\ell_k}^{RL} + f_n^{LR} Y_{i\ell_k}^{RL} Y_{j\ell_k}^{LR}), \tag{A1}$$

where the nonvanishing $f_n^{\cdots}$ coefficients in turn can be cast as

$$f_n^{\cdots} = a_n^{\cdots}(f_{ni}^{\cdots} Q_i^2 + f_{nk}^{\cdots} Q_k^2 + f_{nik}^{\cdots} Q_i Q_k), \tag{A2}$$

with $\ldots$ standing for LL, RR, etc. The $a_n^{\cdots}$ and $f_{n\ldots}^{\cdots}$ coefficients are

$$a_1^{LL} = \frac{1}{\delta_s \hat{s}^2 \delta_t \hat{t}^2}, \tag{A3}$$

$$\begin{aligned} f_{1i}^{LL} = {} & \delta_t(2\delta_s\hat{t}(2\hat{s}(-D_{001}(2) - D_{001}(4) - 2(D_{003}(2) + D_{003}(4)) + C_2(7)) - 2C_{12}(4)\hat{u} + 4C_{00}(4) \\ & + B_0(3)(y_S^2 - y_k^2 - 1)) + \delta_s\hat{s}(4C_{00}(6) + B_0(3)(y_S^2 - y_k^2 - 1)) - 4C_{12}(4)\delta_s\hat{t}^2) \\ & + 2\delta_s\hat{t}^2((B_0(1) + 1)y_k^2 - (B_0(2) + 1)y_S^2 - 2C_{12}(11)\hat{s}) + \delta_s\hat{t}(\hat{s}(4C_{00}(11) - B_0(5)) \\ & + (B_0(1) + 1)y_k^2(\hat{s} - 2) - (B_0(2) + 1)(\hat{s} - 2)y_S^2) + B_0(5)\delta_s\hat{s}(y_S^2 - y_k^2), \end{aligned} \tag{A4}$$

$$f_{1k}^{LL} = \delta_t(2\delta_s\hat{s}\,\hat{t}(-(2(D_{11}(10)+D_{11}(11)+D_{11}(12)+D_{12}(10)+D_{13}(10)+D_{13}(11)+D_{13}(12)) + 2(D_1(10)+D_1(11))+D_1(12)-D_3(12))\hat{u} - 2(D_{00}(9)+2D_{00}(10)+D_{00}(11)+D_{00}(12)+D_{001}(2) + D_{001}(4)+2D_{001}(9)+2(D_{001}(10)-D_{001}(11)-D_{001}(12))+D_{002}(9)+D_{002}(10)+2(D_{003}(2)+D_{003}(4)) + D_{003}(9)+D_{003}(10)-D_{003}(11)-D_{003}(12))+C_0(13)-2C_1(18)+2C_2(7)+D_3(12)\delta_s) - 2(2(D_{11}(10)+D_{11}(11)+D_{11}(12)+D_{12}(11)+D_{12}(12)+D_{13}(10)+D_{13}(11)+2D_{13}(12) + D_{23}(12)+D_{33}(12)+D_1(10)+D_1(11)+D_1(12))+D_3(12))\delta_s\hat{s}\hat{t}^2), \tag{A5}$$

$$f_{1ik}^{LL} = \delta_t(2\delta_s\hat{t}(\hat{s}(2((D_{11}(10)+D_{12}(10)+D_{13}(10)+D_1(10))\hat{u}+D_{00}(9)+D_{002}(9)+D_{002}(10) + 2(D_{00}(10)+D_{001}(2)+D_{001}(4)+D_{001}(9)+D_{001}(10))+4(D_{003}(2)+D_{003}(4))+D_{003}(9)+D_{003}(10) - 2C_2(7))+C_1(17))+2(C_{12}(3)+C_{12}(4))\hat{u}-4(C_{00}(3)+C_{00}(4))+2B_0(3)) + 2\delta_s\hat{s}(B_0(3)-2(C_{00}(5)+C_{00}(6)))+4\delta_s\hat{t}^2(C_{12}(3)+C_{12}(4)+(D_{11}(10)+D_{13}(10)+D_1(10))\hat{s})) + 2\delta_s\hat{s}\,\hat{t}(B_0(5)-2(C_{00}(10)+C_{00}(11)))+4(C_{12}(10)+C_{12}(11))\delta_s\hat{s}\hat{t}^2, \tag{A6}$$

$$a_1^{RL} = -\frac{2y_k}{\hat{s}\,\hat{t}}, \tag{A7}$$

$$f_{1i}^{RL} = -\frac{2}{\hat{s}}(2(D_{00}(2)+D_{00}(4))\hat{s}+B_0(3)(\hat{s}+\hat{u}-2)+B_0(4)-C_0(15)\hat{s}+C_1(16)\hat{u}) + \frac{1}{\delta_t\delta_s(y_k^2-y_S^2)}(\hat{t}(-2(\hat{s}+\hat{u}-2)((B_0(1)+1)y_k^2-(B_0(2)+1)y_S^2)-2C_2(10)\delta_s(y_k^2-y_S^2)) + \hat{t}^2(2(B_0(2)+1)y_S^2-2(B_0(1)+1)y_k^2)+((B_0(1)+1)y_k^2-y_S^2)(\delta_s+2\hat{u})-B_0(2)y_S^2(\hat{s}+2\hat{u}-1)) - \frac{2\hat{t}}{\hat{s}}(B_0(3)+C_1(16))+\frac{1}{\delta_{\hat{t}}\hat{t}}(\delta_{\hat{t}}B_0(3)+B_0(5)), \tag{A8}$$

$$f_{1k}^{RL} = 2(C_0(14)+C_0(15)-D_0(7)\delta_{\hat{s}})-4(D_{00}(2)+D_{00}(4)+D_{00}(9)+D_{00}(10)+D_{00}(11)+D_{00}(12)) + 2(D_1(11)+D_1(12)-D_0(5)-D_1(10)-D_2(1)+D_2(11)+D_2(12)+D_3(11)+D_3(12))\hat{t} - 2(D_0(5)+D_1(10)-D_1(11)-D_1(12)+D_2(1)+D_2(10)-D_3(11))\hat{u}+D_0(8), \tag{A9}$$

$$f_{1ik}^{RL} = 4(2D_{00}(2)+2D_{00}(4)+D_{00}(9)+D_{00}(10))+2\hat{t}\left(\frac{1}{\delta_s}C_0(1)+D_0(5)+D_1(10)+D_2(1)\right)+\frac{2\hat{u}}{\delta_s}C_0(1) - \frac{1}{\delta_t}C_0(2)+\frac{1}{\hat{t}}C_0(13)-2C_0(2)-4C_0(15)+2(D_0(5)+D_1(10)+D_2(1)+D_2(10))\hat{u}, \tag{A10}$$

$$a_2^{RR} = -\frac{4}{\delta_{\hat{t}}\hat{s}\hat{t}^2}, \tag{A11}$$

$$f_{2i}^{RR} = \delta_t(2\hat{t}(C_{22}(6)+2(D_{00}(4)+D_{001}(4)+D_{003}(2)+D_{003}(4))+C_1(17))+4C_{00}(6) + C_{12}(6)(1-2\hat{s}-2\hat{u})+B_0(3)(y_S^2-y_k^2-1))+\hat{t}(4C_{00}(11)+(B_0(1)+1)y_k^2-(B_0(2)+1)y_S^2 - B_0(5))+B_0(5)(y_S^2-y_k^2), \tag{A12}$$

$$f_{2k}^{RR} = \delta_t\hat{t}(-2(D_{11}(9)+D_{11}(11)+D_{11}(12)+D_{12}(9)+D_{13}(9)+D_{13}(11) + D_{13}(12)+D_1(9)+D_1(11)+D_1(12))\hat{s}+4(D_{00}(4)+D_{00}(9)-D_{00}(12))+D_{11}(9)+D_{11}(11)+D_{11}(12) + D_{12}(9)+D_{13}(9)+D_{13}(11)+D_{13}(12)+4(D_{001}(4)+D_{001}(9)+D_{001}(10)-D_{001}(11)-D_{001}(12)+D_{002}(9) + D_{003}(2)+D_{003}(4)+D_{003}(9)-D_{003}(12))+2(D_0(6)+D_1(3)+D_1(9)+D_2(3)+D_2(9))y_k^2 + D_1(9)+D_1(11)+D_1(12)), \tag{A13}$$

$$f_{2ik}^{RR} = \delta_t(\hat{t}(-2(C_{22}(5)+C_{22}(6))+2(D_{11}(9)+D_{12}(9)+D_{13}(9)+D_1(9))\hat{s}$$
$$-4(2D_{00}(4)+D_{00}(9))-D_{11}(9)-D_{12}(9)-D_{13}(9)-4(2D_{001}(4)+D_{001}(9)+D_{001}(10)+D_{002}(9)$$
$$+2(D_{003}(2)+D_{003}(4))+D_{003}(9))-4C_1(17)-2(D_0(6)+D_1(3)+D_1(9)+D_2(3)+D_2(9))y_k^2-D_1(9))$$
$$+(C_{12}(5)+C_{12}(6))(2\hat{s}+2\hat{u}-1)+2B_0(3))+2\hat{t}(B_0(5)-2(C_{00}(5)+C_{00}(6)+C_{00}(10)+C_{00}(11)))$$
$$+4(C_{00}(5)+C_{00}(6)), \tag{A14}$$

$$a_2^{LR} = \frac{4y_k}{\hat{s}\,\hat{t}}, \tag{A15}$$

$$f_{2i}^{LR} = \frac{1}{\hat{t}}(B_0(3)-C_1(17))+\frac{1}{\delta_t}\left(\frac{2}{y_k^2-y_S^2}((B_0(2)+1)y_S^2-(B_0(1)+1)y_k^2)+\frac{2}{\hat{t}}B_0(5)\right), \tag{A16}$$

$$f_{2k}^{LR} = 2D_0(8)-D_0(6)-D_1(9)+D_1(11)+D_1(12)-D_2(3)-D_2(9)+D_3(12), \tag{A17}$$

$$f_{2ki}^{LR} = \frac{2}{\delta_t}C_0(2)+\frac{1}{\hat{t}}C_0(13)+D_0(6)+D_1(9)+D_2(3)+D_2(9), \tag{A18}$$

$$a_3^{LL} = -\frac{4}{\hat{s}\,\hat{t}}, \tag{A19}$$

$$f_{3i}^{LL} = D_{13}(2)+D_{13}(4)+2(D_{33}(2)+D_{33}(4)+D_{333}(2)+D_{333}(4))+D_{113}(2)+D_{113}(4)+3(D_{133}(2)+D_{133}(4)), \tag{A20}$$

$$f_{3k}^{LL} = 2(D_{11}(9)+D_{11}(10))-4(D_{11}(11)-D_{11}(12))+D_{12}(9)+D_{12}(10)+D_{13}(2)$$
$$+D_{13}(4)+D_{13}(9)+D_{13}(10)+2(D_{33}(2)+D_{33}(4)+D_{111}(9)+D_{111}(10)-D_{111}(11)-D_{111}(12))$$
$$-3(D_{13}(11)+D_{13}(12)-D_{112}(9)-D_{112}(10)-D_{113}(9)-D_{113}(10)+D_{113}(11)+D_{113}(12)$$
$$-D_{133}(2)-D_{133}(4))+D_{113}(2)+D_{113}(4)+D_{122}(9)+D_{122}(10)+2(D_{123}(9)+D_{123}(10))+D_{133}(9)$$
$$+D_{133}(10)-D_{133}(11)-D_{133}(12)+2(D_{333}(2)+D_{333}(4))-2D_1(11)-2D_1(12), \tag{A21}$$

$$f_{3ik}^{LL} = -(2(D_{11}(9)+D_{11}(10))+D_{12}(9)+D_{12}(10)+2(D_{13}(2)+D_{13}(4))+D_{13}(9)+D_{13}(10)+4(D_{33}(2)+D_{33}(4))$$
$$+2(D_{111}(9)+D_{111}(10))+3(D_{112}(9)+D_{112}(10))+2(D_{113}(2)+D_{113}(4))+3(D_{113}(9)+D_{113}(10))$$
$$+D_{122}(9)+D_{122}(10)+2(D_{123}(9)+D_{123}(10))+6(D_{133}(2)+D_{133}(4))+D_{133}(9)+D_{133}(10)$$
$$+4(D_{333}(2)+D_{333}(4))), \tag{A22}$$

$$a_3^{RL} = \frac{8y_k}{\hat{s}\,\hat{t}}, \tag{A23}$$

$$f_{3i}^{RL} = D_{13}(2)+D_{13}(4)+D_{33}(2)+D_{33}(4)+D_3(2)+D_3(4), \tag{A24}$$

$$f_{3ik}^{RL} = D_{11}(9)+D_{11}(10)+D_{11}(11)+D_{11}(12)+D_{12}(9)+D_{12}(10)+D_{13}(2)+D_{13}(4)+D_{13}(9)+D_{13}(10)$$
$$+D_{13}(11)+D_{13}(12)+D_{33}(2)+D_{33}(4)+D_1(9)+D_1(10)+D_1(11)+D_1(12)+D_3(2)+D_3(4), \tag{A25}$$

$$f_{3k}^{RL} = -(D_{11}(9)+D_{11}(10)+D_{12}(9)+D_{12}(10)+2(D_{13}(2)+D_{13}(4))+D_{13}(9)+D_{13}(10)+2(D_{33}(2)+D_{33}(4))$$
$$+D_1(9)+D_1(10)+2(D_3(2)+D_3(4))), \tag{A26}$$

$$a_4^{RR} = \frac{1}{\hat{s}\delta_t\hat{t}^2}, \tag{A27}$$

$$f_{4i}^{RR} = \delta_t(4C_{00}(6) + 4(D_{001}(2) - D_{001}(4))\hat{t} + B_0(3)(y_S^2 - y_k^2 - 1)) + \hat{t}(4C_{00}(11) + (B_0(1) + 1)y_k^2 - (B_0(2) + 1)y_S^2 - B_0(5)) + B_0(5)(y_S^2 - y_k^2), \tag{A28}$$

$$f_{4k}^{RR} = 2\delta_t\hat{t}(-2(D_{00}(9) + D_{00}(11) + D_{00}(12) - D_{001}(2) + D_{001}(4) + D_{002}(9) - D_{002}(10) + D_{003}(9) - D_{003}(10) + D_{003}(11) - D_{003}(12)) + C_0(13) + D_1(12)\hat{u}), \tag{A29}$$

$$f_{4ik}^{RR} = 2\hat{t}(B_0(5) - 2(C_{00}(10) + C_{00}(11))) + \delta_t(2(B_0(3) - 2(C_{00}(5) + C_{00}(6))) + 2\hat{t}(2(D_{00}(9) - 2D_{001}(2) + 2D_{001}(4) + D_{002}(9) - D_{002}(10) + D_{003}(9) - D_{003}(10)) + C_1(17))), \tag{A30}$$

$$a_4^{LR} = \frac{2y_k}{\hat{s}\delta_{\hat{t}}\hat{t}^2}, \tag{A31}$$

$$f_{4i}^{LR} = \frac{\hat{t}}{y_k^2 - y_S^2}((B_0(1) + 1)y_k^2 - (B_0(2) + 1)y_S^2) - B_0(5) - B_0(3)\delta_{\hat{t}}, \tag{A32}$$

$$f_{4k}^{LR} = -D_0(8)\hat{t}\delta_{\hat{t}}, \tag{A33}$$

$$f_{4ik}^{LR} = -(C_0(2)\hat{t} + C_0(13)\delta_{\hat{t}}), \tag{A34}$$

$$a_5^{LL} = \frac{4}{\hat{s}\hat{t}^2}, \tag{A35}$$

$$f_{5i}^{LL} = C_{12}(6), \tag{A36}$$

$$f_{5k}^{LL} = \hat{t}(D_{11}(9) + D_{11}(11) + D_{11}(12) + D_{12}(9) + D_{13}(9) + D_{13}(11) + D_{13}(12) + D_1(9) + D_1(11) + D_1(12)), \tag{A37}$$

$$f_{5ik}^{LL} = -(C_{12}(5) + C_{12}(6) + \hat{t}(D_{11}(9) + D_{12}(9) + D_{13}(9) + D_1(9))), \tag{A38}$$

$$a_5^{RL} = -\frac{4y_k}{\hat{s}\hat{t}^2}, \tag{A39}$$

$$f_{5i}^{RL} = C_1(17), \tag{A40}$$

$$f_{5k}^{RL} = \hat{t}(D_0(6) + D_1(9) - D_1(11) - D_1(12) + D_2(3) + D_2(9) - D_3(12)), \tag{A41}$$

$$f_{5ik}^{RL} = C_0(13) - \hat{t}(D_0(6) + D_1(9) + D_2(3) + D_2(9)), \tag{A42}$$

and

$$a_6^{RR} = \frac{4}{\hat{s}\,\hat{t}}, \tag{A43}$$

$$f_{6i}^{RR} = D_{13}(2) - D_{13}(4) + D_{113}(2) - D_{113}(4) + D_{133}(2) - D_{133}(4), \tag{A44}$$

$$f_{6k}^{RR} = -D_{12}(9) + D_{12}(10) + D_{13}(2) - D_{13}(4) - D_{13}(9) + D_{13}(10) - D_{13}(11) + D_{13}(12) - D_{112}(9) + D_{112}(10) + D_{113}(2) - D_{113}(4) - D_{113}(9) + D_{113}(10) - D_{113}(11) + D_{113}(12) - D_{122}(9) + D_{122}(10) - 2D_{123}(9) + 2D_{123}(10) + D_{133}(2) - D_{133}(4) - D_{133}(9) + D_{133}(10) - D_{133}(11) + D_{133}(12), \tag{A45}$$

$$f_{6ik}^{RR} = D_{12}(9) - D_{12}(10) - 2D_{13}(2) + 2D_{13}(4) + D_{13}(9) - D_{13}(10) + D_{112}(9) - D_{112}(10) - 2D_{113}(2) + 2D_{113}(4) + D_{113}(9) - D_{113}(10) + D_{122}(9) - D_{122}(10) + 2D_{123}(9) - 2D_{123}(10) - 2D_{133}(2) + 2D_{133}(4) + D_{133}(9) - D_{133}(10). \tag{A46}$$

TABLE IV. Arguments of the two-point scalar functions $B_0(i)$ in the notation of [173].

(i)	(a, b, c)
(1)	$(0, m_k^2, m_k^2)$
(2)	$(0, m_S^2, m_S^2)$
(3)	(m_i^2, m_k^2, m_S^2)
(4)	(s, m_k^2, m_S^2)
(5)	(t, m_k^2, m_S^2)

As far as the arguments of the Passarino-Veltman scalar functions and tensor integral coefficients are concerned, they are presented in Tables IV through VI, where again we follow the notation of [173].

APPENDIX B: AVERAGE SQUARE AMPLITUDE FOR THE $f_i \to f_j\gamma\gamma$ DECAY

After averaging (summing) over polarizations of the ingoing fermion (outgoing particles), from Eq. (12) we

TABLE V. Arguments of the three-point scalar functions $C_0(i)$ and three-point tensor integral coefficients $C_j(i)$ and $C_{jk}(i)$ in the notation of [173].

(i)	(a, b, c, d, e, f, g)
(1)	$(0,0,s,m_k^2,m_k^2,m_S^2)$
(2)	$(0,0,t,m_k^2,m_k^2,m_S^2)$
(3)	$(0,m_i^2,s,m_k^2,m_k^2,m_S^2)$
(4)	$(0,m_i^2,s,m_S^2,m_S^2,m_k^2)$
(5)	$(0,m_i^2,t,m_k^2,m_k^2,m_S^2)$
(6)	$(0,m_i^2,t,m_S^2,m_S^2,m_k^2)$
(7)	$(0,m_i^2,u,m_S^2,m_k^2,m_S^2)$
(8)	$(0,s,0,m_k^2,m_k^2,m_S^2)$
(9)	$(0,s,0,m_S^2,m_S^2,m_k^2)$
(10)	$(0,t,0,m_k^2,m_k^2,m_S^2)$
(11)	$(0,t,0,m_S^2,m_S^2,m_k^2)$
(12)	$(m_i^2,0,s,m_S^2,m_k^2,m_k^2)$
(13)	$(m_i^2,0,t,m_S^2,m_k^2,m_k^2)$
(14)	$(m_i^2,0,u,m_k^2,m_S^2,m_k^2)$
(15)	$(m_i^2,0,u,m_S^2,m_k^2,m_S^2)$
(16)	$(m_i^2,s,0,m_k^2,m_S^2,m_k^2)$
(17)	$(m_i^2,t,0,m_k^2,m_S^2,m_k^2)$
(18)	$(m_i^2,u,0,m_S^2,m_k^2,m_k^2)$

TABLE VI. Arguments of the four-point scalar functions $D_0(i)$ and four-point tensor integral coefficients $D_j(i)$, $D_{jk}(i)$, and $D_{jkl}(i)$ in the notation of [173].

(i)	(a, b, c, d, e, f, g, h, i, j)
(1)	$(0,s,0,t,0,m_i^2,m_k^2,m_k^2,m_S^2,m_S^2)$
(2)	$(0,s,m_i^2,u,0,0,m_S^2,m_S^2,m_k^2,m_S^2)$
(3)	$(0,t,0,s,0,m_i^2,m_k^2,m_k^2,m_S^2,m_S^2)$
(4)	$(0,t,m_i^2,u,0,0,m_S^2,m_S^2,m_k^2,m_S^2)$
(5)	$(m_i^2,0,0,0,s,t,m_k^2,m_S^2,m_S^2,m_k^2)$
(6)	$(m_i^2,0,0,0,s,t,m_S^2,m_k^2,m_k^2,m_S^2)$
(7)	$(m_i^2,0,0,0,s,u,m_S^2,m_k^2,m_k^2,m_k^2)$
(8)	$(m_i^2,0,0,0,t,u,m_S^2,m_k^2,m_k^2,m_k^2)$
(9)	$(m_i^2,s,0,t,0,0,m_k^2,m_S^2,m_k^2,m_S^2)$
(10)	$(m_i^2,t,0,s,0,0,m_k^2,m_S^2,m_k^2,m_S^2)$
(11)	$(m_i^2,u,0,s,0,0,m_S^2,m_k^2,m_k^2,m_k^2)$
(12)	$(m_i^2,u,0,t,0,0,m_S^2,m_k^2,m_k^2,m_k^2)$

obtain the following average square amplitude in the $m_j \simeq 0$ limit:

$$|\bar{\mathcal{M}}(f_i \to f_j\gamma\gamma)|^2 = \frac{N_c^2\alpha^2}{16\pi^2}(\mathcal{A}_1 + \mathcal{A}_2), \tag{B1}$$

with

$$\begin{aligned}\mathcal{A}_1 = \Big\{ & \frac{\hat{s}\,\hat{t}}{32}[(\hat{s}+\hat{t})(4\hat{s}\|F_1\|^2 + 2\hat{t}\,\hat{u}\,\|F_2\|^2 + \hat{s}\hat{u}^2\|F_3\|^2) \\ & + ((\hat{s}-\hat{t})^2 + \hat{u}(\hat{s}+\hat{t}))(4\hat{s}\|F_4\|^2 + 2\hat{t}\,\hat{u}\,\|F_5\|^2 + \hat{s}\hat{u}^2\|F_6\|^2) + 2\hat{s}(\hat{s}+\hat{t})\hat{u}\mathrm{Re}(F_1F_3^*) \\ & + \hat{u}((\hat{s}-\hat{t})^2 - (\hat{s}+\hat{t})^2)\mathrm{Re}((2F_1+\hat{u}F_3)F_5^* - F_2(2F_4^* + \hat{u}F_6^*)) + 2\hat{s}\,\hat{u}\,((\hat{s}-\hat{t})^2 + \hat{u}(\hat{s}+\hat{t}))\mathrm{Re}(F_4F_6^*) \\ & + 2\hat{t}(\hat{t}-\hat{s})\mathrm{Re}(\hat{s}(4F_1+\hat{u}F_3)F_4^* + 2\hat{t}\,\hat{u}\,F_2F_5^* + \hat{s}\,\hat{u}(F_1+\hat{u}F_3)F_6^*)] + (\hat{s}\leftrightarrow\hat{t})\Big\} + (Y_{lk}^{LR} \leftrightarrow Y_{lk}^{RL}),\end{aligned}$$

and

$$\begin{aligned}\mathcal{A}_2 = \frac{1}{32}\hat{s}\hat{t}^2\mathrm{Re}\Big[& 2\hat{s}(\hat{s}+\hat{t})\hat{u}(F_3G_1^* - F_2G_2^* + F_1G_3^* + \hat{u}F_3G_3^*) \\ & + \hat{u}^2((\hat{s}-\hat{t})^2 - (\hat{s}+\hat{t})^2)\left(\frac{\hat{s}}{\hat{t}}(F_6G_2^* + F_3G_5^*) + F_5G_3^* + F_2G_6^*\right) \\ & + 2\hat{s}\,\hat{u}\,((\hat{s}-\hat{t})^2 + \hat{u}(\hat{s}+\hat{t}))(F_5G_5^* - F_6G_6^* - F_6G_4^* - F_4G_6^*) \\ & + 2\hat{s}\,\hat{u}\,(\hat{t}-\hat{s})(F_6G_1^* - F_1G_6^* + F_2G_5^* - F_5G_2^* + F_4G_3^* - F_3G_4^* + \hat{u}F_6G_3^* - \hat{u}F_3G_6^*)\Big] + (\hat{s}\leftrightarrow\hat{t}),\end{aligned} \tag{B2}$$

where $G_n(\hat{s},\hat{t}) = F_n(\hat{t},\hat{s})$ are the form factors obtained after exchanging the photons. The extra terms arise from the right-handed amplitude $\mathcal{M}_R$ and interference terms.

APPENDIX C: LQ CONTRIBUTION TO LEPTON PROCESS

For completeness we present some formulas used in the evaluation of the constraints on the LQ couplings presented in Sec. IV B.

1. Muon anomalous magnetic dipole moment

The one-loop contribution to the muon anomalous magnetic dipole moment a_μ^{LQ} from a charge Q_S scalar LQ with couplings to the muon and quark q_i can be written as [135]

$$\begin{aligned}a_\mu^{\mathrm{LQ}} = -\sum_i \frac{3\sqrt{x_\mu}}{32\pi^2}(& \sqrt{x_\mu}(|Y_{i\mu}^{RL}|^2 + |Y_{i\mu}^{LR}|^2)F(x_\mu, x_{q_i}) \\ & + 2\sqrt{x_{q_i}}\mathrm{Re}(Y_{i\mu}^{RL}Y_{i\mu}^{LR*})G(x_\mu, x_{q_i})),\end{aligned} \tag{C1}$$

where $x_a = m_a^2/m_S^2$ and the sum runs over the second and third generation up (down) quarks for $Q_S = 5/3$ ($Q_S = 2/3$). The $F(x,y)$ and $G(x,y)$ functions are given in terms of Feynman parameter integrals by

$$F(z_1,z_2) = 2\int_0^1 \frac{(1-x)x(Q_{q_i}(1-x)+Q_S x)}{(1-x)(z_2-xz_1)+x}\,dx, \quad \text{(C2)}$$

$$G(z_1,z_2) = 2\int_0^1 \frac{(1-x)(Q_{q_i}(1-x)+Q_S x)}{(1-x)(z_2-xz_1)+x}\,dx, \quad \text{(C3)}$$

where the electric charges of the internal quark and the LQ q_i and Q_S are in units of the positron charge. In the limit of a heavy quark, $a_\mu^{\rm LQ}$ reduces to

$$a_\mu^{\rm LQ} \simeq \frac{3}{16\pi^2}\sum_i \frac{\sqrt{x_\mu}\sqrt{x_{q_i}}}{(1-x_{q_i})^3}\,{\rm Re}(Y_{i\mu}^{RL}Y_{i\mu}^{LR*}) \times (Q_{q_i}(3-4x_{q_i}+x_{q_i}^2+2\log(x_{q_i})) - Q_S(1-x_{q_i}^2+2x_{q_i}\log(x_{q_i}))). \quad \text{(C4)}$$

We note that since $\Omega_{2/3}$ is a chiral LQ (it only has either left- or right-handed couplings to fermion pairs), its contribution to a_μ can be neglected as it is proportional to x_μ rather than $\sqrt{x_\mu}\sqrt{x_{q_i}}$.

2. $\tau \to \mu\gamma$ decay

A charge Q_S scalar LQ contributes at the one-loop level to the $\tau \to \mu\gamma$ decay via triangle diagrams with an internal LQ. The corresponding decay width is given by

$$\Gamma(\tau\to\mu\gamma) = \frac{m_\tau}{16\pi}\left(1-\left(\frac{m_\mu}{m_\tau}\right)^2\right)^3(|L|^2+|R|^2), \quad \text{(C5)}$$

where the L and R form factors are ultraviolet finite and are given in terms of Feynman parameter integrals as follows [135]:

$$L = \frac{3g^2 e\sqrt{x_\tau}}{64c_W^2\pi^2}\sum_i(\sqrt{x_\tau}Y_{i\tau}^{RL}Y_{i\mu}^{RL}H_1(x_{q_i}) + \sqrt{x_\mu}Y_{i\tau}^{LR}Y_{i\mu}^{LR}H_2(x_{q_i}) + \sqrt{x_{q_i}}Y_{i\mu}^{RL}Y_{i\tau}^{LR}H_3(x_{q_i})), \quad \text{(C6)}$$

where

$$H_1(z) = \int_0^1 dx\int_0^{1-x} dyx\left(\frac{Q_{q_i}y}{\zeta_1(x_\tau,x_\mu,z)} - \frac{Q_S(1-x-y)}{\zeta_2(x_\tau,x_\mu,z)}\right), \quad \text{(C7)}$$

$$H_2(z) = \int_0^1 dx\int_0^{1-x} dy(1-x-y) \times\left(\frac{Q_{q_i}x}{\zeta_1(x_\tau,x_\mu,z)} - \frac{Q_S y}{\zeta_2(x_\tau,x_\mu,z)}\right), \quad \text{(C8)}$$

and

$$H_3(z) = \int_0^1 dx\int_0^{1-x} dy\left(\frac{Q_{q_i}(1-x)}{\zeta_1(x_\tau,x_\mu,z)} - \frac{Q_S(1-x-y)}{\zeta_2(x_\tau,x_\mu,z)}\right), \quad \text{(C9)}$$

with

$$\zeta_1(z_1,z_2,z_3) = x(y(z_1-z_2)+z_2(x-1)+1-z_3) + z_3, \quad \text{(C10)}$$

$$\zeta_2(z_1,z_2,z_3) = xy(z_2-z_1) - x((1-x)z_1-z_3-1) - y((1-y)z_2-z_3-1)+z_3. \quad \text{(C11)}$$

In addition, the right-handed form factor can be obtained from the left-handed one as follows:

$$R = L\begin{pmatrix} Y_{m\ell_k}^{RL} \leftrightarrow Y_{m\ell_k}^{LR} \\ Q_S \to -Q_S \end{pmatrix}. \quad \text{(C12)}$$

We note that the results presented in this appendix are given in terms of Passarino-Veltman scalar functions in [135].

[1] D. Chakraborty, J. Konigsberg, and D. L. Rainwater, Review of top quark physics, Annu. Rev. Nucl. Part. Sci. **53**, 301 (2003).

[2] F. Larios, R. Martinez, and M. Perez, New physics effects in the flavor-changing neutral couplings of the top quark, Int. J. Mod. Phys. A **21**, 3473 (2006).

[3] G. Eilam, J. Hewett, and A. Soni, Rare decays of the top quark in the standard and two Higgs doublet models, Phys. Rev. D **44**, 1473 (1991).

[4] J. Diaz-Cruz, R. Martinez, M. Perez, and A. Rosado, Flavor changing radiative decay of the t quark, Phys. Rev. D **41**, 891 (1990).

[5] G.-R. Lu, Y. Hua, X.-L. Wang, J.-M. Yang, and W.-Q. Sun, Rare decays of the top quark in the technicolour model with a massless scalar doublet, J. Phys. G **22**, 305 (1996).

[6] X.-L. Wang, G.-R. Lu, J.-M. Yang, Z.-J. Xiao, C.-X. Yue, and Y. Zhang, Rare decays of the top quark in the one generation technicolor model, Phys. Rev. D **50**, 5781 (1994).

[7] G.-R. Lu, C.-X. Yue, and J.-S. Huang, Rare decays of the top quark in the top-color-assisted multiscale technicolor model, Phys. Rev. D **57**, 1755 (1998).

[8] G.-r. Lu, F.-r. Yin, X.-l. Wang, and L.-d. Wan, The rare top quark decays $\vec{t} \times cV$ in the topcolor assisted technicolor model, Phys. Rev. D **68**, 015002 (2003).

[9] G. Couture, C. Hamzaoui, and H. Konig, Flavor changing top quark decay within the minimal supersymmetric Standard Model, Phys. Rev. D **52**, 1713 (1995).

[10] C. S. Li, R. Oakes, and J. M. Yang, Rare decay of the top quark in the minimal supersymmetric model, Phys. Rev. D **49**, 293 (1994).

[11] J. L. Lopez, D. V. Nanopoulos, and R. Rangarajan, New supersymmetric contributions to $\vec{t} \times cV$, Phys. Rev. D **56**, 3100 (1997).

[12] J. M. Yang, B.-L. Young, and X. Zhang, Flavor changing top quark decays in R-parity violating SUSY, Phys. Rev. D **58**, 055001 (1998).

[13] M. Frank and I. Turan, $t \to cg$, $c\gamma$, cZ in the left-right supersymmetric model, Phys. Rev. D **72**, 035008 (2005).

[14] G. Gonzalez-Sprinberg, R. Martinez, and J. A. Rodriguez, FCNC top quark decays in extra dimensions, Eur. Phys. J. C **51**, 919 (2007).

[15] A. Cordero-Cid, G. Tavares-Velasco, and J. Toscano, Effects of an extra Z' gauge boson on the top quark decay $t \to c\gamma$, Phys. Rev. D **72**, 057701 (2005).

[16] A. Cordero-Cid, M. Perez, G. Tavares-Velasco, and J. Toscano, Effective Lagrangian approach to Higgs-mediated FCNC top quark decays, Phys. Rev. D **70**, 074003 (2004).

[17] I. Cortés-Maldonado, G. Hernández-Tomé, and G. Tavares-Velasco, Decay $t \to c\gamma$ in models with $SU_L(3) \times U_X(1)$ gauge symmetry, Phys. Rev. D **88**, 014011 (2013).

[18] J. L. Diaz-Cruz, M. A. Perez, G. Tavares-Velasco, and J. J. Toscano, Testing flavor changing neutral currents in the rare top quark decays $\vec{t}cV_iV_j$, Phys. Rev. D **60**, 115014 (1999).

[19] J. Han, B. Li, and X. Wang, Top quark rare three-body decays in the littlest Higgs model with T-parity, Phys. Rev. D **83**, 034032 (2011).

[20] J. Han, B. Yang, and J. Li, Revisiting rare top quark decays in the littlest Higgs Model with T-parity, Int. J. Mod. Phys. A **31**, 1650165 (2016).

[21] C.-x. Yue, G.-r. Lu, Q.-j. Xu, G.-l. Liu, and G.-p. Gao, The Flavor changing rare top decays $t \to c \times VV$ in topcolor assisted technicolor theory, Phys. Lett. B **508**, 290 (2001).

[22] A. Bolaños, R. Sánchez-Vélez, and G. Tavares-Velasco, Flavor changing neutral current decays $t \to cX$ ($X = \gamma$, g, Z, H) and $t \to c\bar{\ell}\ell$ ($\ell = \mu$, τ) via scalar leptoquarks, Eur. Phys. J. C **79**, 700 (2019).

[23] J. C. Pati and A. Salam, Lepton number as the fourth color, Phys. Rev. D **10**, 275 (1974); **11**, 703(E) (1975).

[24] H. Georgi and S. L. Glashow, Unity of All Elementary Particle Forces, Phys. Rev. Lett. **32**, 438 (1974).

[25] H. Georgi, H. R. Quinn, and S. Weinberg, Hierarchy of Interactions in Unified Gauge Theories, Phys. Rev. Lett. **33**, 451 (1974).

[26] H. Fritzsch and P. Minkowski, Unified interactions of leptons and hadrons, Ann. Phys. (N.Y.) **93**, 193 (1975).

[27] S. Dimopoulos, S. Raby, and L. Susskind, Light composite fermions, Nucl. Phys. **B173**, 208 (1980).

[28] G. Senjanovic and A. Sokorac, Light leptoquarks in SO(10), Z. Phys. C **20**, 255 (1983).

[29] P. H. Frampton and B.-H. Lee, SU(15) Grand Unification, Phys. Rev. Lett. **64**, 619 (1990).

[30] B. Schrempp and F. Schrempp, Light leptoquarks, Phys. Lett. **153B**, 101 (1985).

[31] W. Buchmuller, Composite quarks and leptons, Acta Phys. Aust. Suppl. **27**, 517 (1985).

[32] B. Gripaios, Composite leptoquarks at the LHC, J. High Energy Phys. 02 (2010) 045.

[33] E. Witten, Symmetry breaking patterns in superstring models, Nucl. Phys. **B258**, 75 (1985).

[34] J. L. Hewett and T. G. Rizzo, Low-energy phenomenology of superstring inspired E(6) models, Phys. Rep. **183**, 193 (1989).

[35] J. R. Ellis, M. K. Gaillard, D. V. Nanopoulos, and P. Sikivie, Can one tell technicolor from a hole in the ground?, Nucl. Phys. **B182**, 529 (1981).

[36] E. Farhi and L. Susskind, Technicolor, Phys. Rep. **74**, 277 (1981).

[37] C. T. Hill and E. H. Simmons, Strong dynamics and electroweak symmetry breaking, Phys. Rep. **381**, 235 (2003); **390**, 553(E) (2004).

[38] P. Langacker, Grand unified theories and proton decay, Phys. Rep. **72**, 185 (1981).

[39] S. Davidson, D. C. Bailey, and B. A. Campbell, Model independent constraints on leptoquarks from rare processes, Z. Phys. C **61**, 613 (1994).

[40] O. U. Shanker, $\pi\ell 2$, $K\ell 3$ and $K^0 - \bar{K}0$ constraints on leptoquarks and supersymmetric particles, Nucl. Phys. **B204**, 375 (1982).

[41] O. U. Shanker, Flavor violation, scalar particles and leptoquarks, Nucl. Phys. **B206**, 253 (1982).

[42] M. Leurer, Bounds on vector leptoquarks, Phys. Rev. D **50**, 536 (1994).

[43] M. Leurer, A comprehensive study of leptoquark bounds, Phys. Rev. D **49**, 333 (1994).

[44] A. Crivellin, D. Müller, and L. Schnell, Combined constraints on first generation leptoquarks, Phys. Rev. D **103**, 115023 (2021); **104**, 055020(A) (2021).

[45] I. Doršner, S. Fajfer, A. Greljo, J. F. Kamenik, and N. Košnik, Physics of leptoquarks in precision experiments and at particle colliders, Phys. Rep. **641**, 1 (2016).

[46] Y. Sakaki, M. Tanaka, A. Tayduganov, and R. Watanabe, Testing leptoquark models in $\bar{B} \to D^{(*)}\tau\bar{\nu}$, Phys. Rev. D **88**, 094012 (2013).

[47] D. Bečirević and O. Sumensari, A leptoquark model to accommodate $R_K^{\rm exp} < R_K^{\rm SM}$ and $R_{K^*}^{\rm exp} < R_{K^*}^{\rm SM}$, J. High Energy Phys. 08 (2017) 104.

[48] A. Crivellin, D. Müller, and T. Ota, Simultaneous explanation of $R(D^{(*)})$ and $bs\mu^+\mu^-$: The last scalar leptoquarks standing, J. High Energy Phys. 09 (2017) 040.

[49] D. Bečirević, I. Doršner, S. Fajfer, N. Košnik, D. A. Faroughy, and O. Sumensari, Scalar leptoquarks from grand unified theories to accommodate the B-physics anomalies, Phys. Rev. D **98**, 055003 (2018).

[50] A. Angelescu, D. Bečirević, D. A. Faroughy, and O. Sumensari, Closing the window on single leptoquark solutions to the B-physics anomalies, J. High Energy Phys. 10 (2018) 183.

[51] D. Buttazzo, A. Greljo, G. Isidori, and D. Marzocca, B-physics anomalies: A guide to combined explanations, J. High Energy Phys. 11 (**2017**) 044.

[52] D. Marzocca and S. Trifinopoulos, Minimal Explanation of Flavor Anomalies: B-Meson Decays, Muon Magnetic Moment, and the Cabibbo Angle, Phys. Rev. Lett. **127**, 061803 (2021).

[53] A. Angelescu, D. Bečirević, D. A. Faroughy, F. Jaffredo, and O. Sumensari, Single leptoquark solutions to the B-physics anomalies, Phys. Rev. D **104**, 055017 (2021).

[54] M. Bauer and M. Neubert, Minimal Leptoquark Explanation for the $R_{D^{(*)}}$, R_K, and $(g-2)_\mu$ Anomalies, Phys. Rev. Lett. **116**, 141802 (2016).

[55] D. Bečirević, S. Fajfer, N. Košnik, and O. Sumensari, Leptoquark model to explain the B-physics anomalies, R_K and R_D, Phys. Rev. D **94**, 115021 (2016).

[56] J. Kumar, D. London, and R. Watanabe, Combined explanations of the $b \to s\mu^+\mu^-$ and $b \to c\tau^-\bar{\nu}$ anomalies: A general model analysis, Phys. Rev. D **99**, 015007 (2019).

[57] K. Cheung, W.-Y. Keung, and P.-Y. Tseng, Isodoublet vector leptoquark solution to the muon $g-2$, $R_{K,K*}$, $R_{D,D*}$, and W-mass anomalies, Phys. Rev. D **106**, 015029 (2022).

[58] A. Bhaskar, A. A. Madathil, T. Mandal, and S. Mitra, Combined explanation of W-mass, muon $g-2$, $R_{K(*)}$ and $R_{D(*)}$ anomalies in a singlet-triplet scalar leptoquark model, Phys. Rev. D **106**, 115009 (2022).

[59] A. Datta, J. L. Feng, S. Kamali, and J. Kumar, Resolving the $(g-2)_\mu$ and B anomalies with leptoquarks and a dark Higgs boson, Phys. Rev. D **101**, 035010 (2020).

[60] C. Hati, J. Kriewald, J. Orloff, and A. M. Teixeira, A nonunitary interpretation for a single vector leptoquark combined explanation to the B-decay anomalies, J. High Energy Phys. 12 (2019) 006.

[61] L. Da Rold and F. Lamagna, A vector leptoquark for the B-physics anomalies from a composite GUT, J. High Energy Phys. 12 (2019) 112.

[62] C. Cornella, J. Fuentes-Martin, and G. Isidori, Revisiting the vector leptoquark explanation of the B-physics anomalies, J. High Energy Phys. 07 (2019) 168.

[63] T. Mandal, S. Mitra, and S. Raz, $R_{D^{(*)}}$ motivated $\mathcal{S}_1$ leptoquark scenarios: Impact of interference on the exclusion limits from LHC data, Phys. Rev. D **99**, 055028 (2019).

[64] R. Alonso, B. Grinstein, and J. Martin Camalich, Lepton universality violation and lepton flavor conservation in B-meson decays, J. High Energy Phys. 10 (2015) 184.

[65] L. Calibbi, A. Crivellin, and T. Ota, Effective Field Theory Approach to $b \to s\ell\ell^{(\prime)}$, $B \to K^{(*)}\nu\bar{\nu}$ and $B \to D^{(*)}\tau\nu$ with Third Generation Couplings, Phys. Rev. Lett. **115**, 181801 (2015).

[66] G. Hiller, D. Loose, and K. Schönwald, Leptoquark flavor patterns & B decay anomalies, J. High Energy Phys. 12 (2016) 027.

[67] B. Bhattacharya, A. Datta, J.-P. Guévin, D. London, and R. Watanabe, Simultaneous explanation of the R_K and $R_{D^{(*)}}$ puzzles: A model analysis, J. High Energy Phys. 01 (2017) 015.

[68] R. Barbieri, G. Isidori, A. Pattori, and F. Senia, Anomalies in B-decays and $U(2)$ flavour symmetry, Eur. Phys. J. C **76**, 67 (2016).

[69] R. Barbieri, C. W. Murphy, and F. Senia, B-decay anomalies in a composite leptoquark model, Eur. Phys. J. C **77**, 8 (2017).

[70] L. Calibbi, A. Crivellin, and T. Li, Model of vector leptoquarks in view of the B-physics anomalies, Phys. Rev. D **98**, 115002 (2018).

[71] A. Crivellin, D. Müller, A. Signer, and Y. Ulrich, Correlating lepton flavor universality violation in B decays with $\mu \to e\gamma$ using leptoquarks, Phys. Rev. D **97**, 015019 (2018).

[72] M. Bordone, C. Cornella, J. Fuentes-Martín, and G. Isidori, Low-energy signatures of the PS^3 model: From B-physics anomalies to LFV, J. High Energy Phys. 10 (2018) 148.

[73] A. Crivellin, C. Greub, D. Müller, and F. Saturnino, Importance of Loop Effects in Explaining the Accumulated Evidence for New Physics in B Decays with a Vector Leptoquark, Phys. Rev. Lett. **122**, 011805 (2019).

[74] M. Bordone, O. Catà, and T. Feldmann, Effective theory approach to new physics with flavour: General framework and a leptoquark example, J. High Energy Phys. 01 (2020) 067.

[75] J. Bernigaud, I. de Medeiros Varzielas, and J. Talbert, Finite family groups for fermionic and leptoquark mixing patterns, J. High Energy Phys. 01 (2020) 194.

[76] J. Aebischer, A. Crivellin, and C. Greub, QCD improved matching for semileptonic B decays with leptoquarks, Phys. Rev. D **99**, 055002 (2019).

[77] J. Fuentes-Martín, G. Isidori, M. König, and N. Selimović, Vector leptoquarks beyond tree level, Phys. Rev. D **101**, 035024 (2020).

[78] O. Popov, M. A. Schmidt, and G. White, R_2 as a single leptoquark solution to $R_{D^{(*)}}$ and $R_{K^{(*)}}$, Phys. Rev. D **100**, 035028 (2019).

[79] S. Fajfer and N. Košnik, Vector leptoquark resolution of R_K and $R_{D^{(*)}}$ puzzles, Phys. Lett. B **755**, 270 (2016).

[80] M. Blanke and A. Crivellin, B Meson Anomalies in a Pati-Salam Model within the Randall-Sundrum Background, Phys. Rev. Lett. **121**, 011801 (2018).

[81] I. de Medeiros Varzielas and J. Talbert, Simplified models of flavourful leptoquarks, Eur. Phys. J. C **79**, 536 (2019).

[82] I. de Medeiros Varzielas and G. Hiller, Clues for flavor from rare lepton and quark decays, J. High Energy Phys. 06 (2015) 072.

[83] A. Crivellin, D. Müller, and F. Saturnino, Flavor phenomenology of the leptoquark singlet-triplet model, J. High Energy Phys. 06 (2020) 020.

[84] S. Saad, Combined explanations of $(g-2)_\mu$, $R_{D^{(*)}}$, $R_{K^{(*)}}$ anomalies in a two-loop radiative neutrino mass model, Phys. Rev. D **102**, 015019 (2020).

[85] S. Saad and A. Thapa, Common origin of neutrino masses and $R_{D^{(*)}}$, $R_{K^{(*)}}$ anomalies, Phys. Rev. D **102**, 015014 (2020).

[86] L. Da Rold and F. Lamagna, Model for the singlet-triplet leptoquarks, Phys. Rev. D **103**, 115007 (2021).

[87] M. Bordone, C. Cornella, J. Fuentes-Martin, and G. Isidori, A three-site gauge model for flavor hierarchies and flavor anomalies, Phys. Lett. B **779**, 317 (2018).

[88] A. Biswas, D. Kumar Ghosh, N. Ghosh, A. Shaw, and A. K. Swain, Collider signature of U_1 leptoquark and constraints from $b \to c$ observables, J. Phys. G **47**, 045005 (2020).

[89] J. Heeck and D. Teresi, Pati-Salam explanations of the B-meson anomalies, J. High Energy Phys. 12 (2018) 103.

[90] S. Sahoo and R. Mohanta, Scalar leptoquarks and the rare B meson decays, Phys. Rev. D **91**, 094019 (2015).

[91] C.-H. Chen, T. Nomura, and H. Okada, Explanation of $B \to K^{(*)}\ell^+\ell^-$ and muon $g-2$, and implications at the LHC, Phys. Rev. D **94**, 115005 (2016).

[92] U. K. Dey, D. Kar, M. Mitra, M. Spannowsky, and A. C. Vincent, Searching for leptoquarks at IceCube and the LHC, Phys. Rev. D **98**, 035014 (2018).

[93] B. Chauhan, B. Kindra, and A. Narang, Discrepancies in simultaneous explanation of flavor anomalies and IceCube PeV events using leptoquarks, Phys. Rev. D **97**, 095007 (2018).

[94] S. Fajfer, J. F. Kamenik, I. Nisandzic, and J. Zupan, Implications of Lepton Flavor Universality Violations in B Decays, Phys. Rev. Lett. **109**, 161801 (2012).

[95] M. Freytsis, Z. Ligeti, and J. T. Ruderman, Flavor models for $\bar{B} \to D^{(*)}\tau\bar{\nu}$, Phys. Rev. D **92**, 054018 (2015).

[96] X.-Q. Li, Y.-D. Yang, and X. Zhang, Revisiting the one leptoquark solution to the $\mathrm{R}(\mathrm{D}^{(*)})$ anomalies and its phenomenological implications, J. High Energy Phys. 08 (2016) 054.

[97] J. Zhu, H.-M. Gan, R.-M. Wang, Y.-Y. Fan, Q. Chang, and Y.-G. Xu, Probing the R-parity violating supersymmetric effects in the exclusive $b \to c\ell^-\bar{\nu}_\ell$ decays, Phys. Rev. D **93**, 094023 (2016).

[98] O. Popov and G. A. White, One Leptoquark to unify them? Neutrino masses and unification in the light of $(g-2)_\mu$, $R_{D^{(\star)}}$ and R_K anomalies, Nucl. Phys. **B923**, 324 (2017).

[99] N. G. Deshpande and X.-G. He, Consequences of R-parity violating interactions for anomalies in $\bar{B} \to D^{(*)}\tau\bar{\nu}$ and $b \to s\mu^+\mu^-$, Eur. Phys. J. C **77**, 134 (2017).

[100] D. Bečirević, N. Košnik, O. Sumensari, and R. Zukanovich Funchal, Palatable leptoquark scenarios for lepton flavor violation in exclusive $b \to s\ell_1\ell_2$ modes, J. High Energy Phys. 11 (2016) 035.

[101] Y. Cai, J. Gargalionis, M. A. Schmidt, and R. R. Volkas, Reconsidering the one leptoquark solution: Flavor anomalies and neutrino mass, J. High Energy Phys. 10 (2017) 047.

[102] W. Altmannshofer, P. S. Bhupal Dev, and A. Soni, $R_{D^{(*)}}$ anomaly: A possible hint for natural supersymmetry with R-parity violation, Phys. Rev. D **96**, 095010 (2017).

[103] S. Kamali, A. Rashed, and A. Datta, New physics in inclusive $B \to X_c\ell\bar{\nu}$ decay in light of $R(D^{(*)})$ measurements, Phys. Rev. D **97**, 095034 (2018).

[104] A. Azatov, D. Bardhan, D. Ghosh, F. Sgarlata, and E. Venturini, Anatomy of $b \to c\tau\nu$ anomalies, J. High Energy Phys. 11 (2018) 187.

[105] T. J. Kim, P. Ko, J. Li, J. Park, and P. Wu, Correlation between $R_{D^{(*)}}$ and top quark FCNC decays in leptoquark models, J. High Energy Phys. 07 (2019) 025.

[106] U. Aydemir, T. Mandal, and S. Mitra, Addressing the $\mathbf{R}_{D^{(*)}}$ anomalies with an $\mathbf{S}_1$ leptoquark from $\mathbf{SO(10)}$ grand unification, Phys. Rev. D **101**, 015011 (2020).

[107] H. Yan, Y.-D. Yang, and X.-B. Yuan, Phenomenology of $b \to c\tau\bar{\nu}$ decays in a scalar leptoquark model, Chin. Phys. C **43**, 083105 (2019).

[108] D. Marzocca, Addressing the B-physics anomalies in a fundamental composite Higgs model, J. High Energy Phys. 07 (2018) 121.

[109] I. Bigaran, J. Gargalionis, and R. R. Volkas, A near-minimal leptoquark model for reconciling flavour anomalies and generating radiative neutrino masses, J. High Energy Phys. 10 (2019) 106.

[110] P. S. Bhupal Dev, R. Mohanta, S. Patra, and S. Sahoo, Unified explanation of flavor anomalies, radiative neutrino masses, and ANITA anomalous events in a vector leptoquark model, Phys. Rev. D **102**, 095012 (2020).

[111] W. Altmannshofer, P. S. B. Dev, A. Soni, and Y. Sui, Addressing $\mathrm{R}_{D^{(*)}}$, $\mathrm{R}_{K^{(*)}}$, muon $g-2$ and ANITA anomalies in a minimal R-parity violating supersymmetric framework, Phys. Rev. D **102**, 015031 (2020).

[112] J. Fuentes-Martín and P. Stangl, Third-family quark-lepton unification with a fundamental composite Higgs, Phys. Lett. B **811**, 135953 (2020).

[113] V. Gherardi, D. Marzocca, and E. Venturini, Low-energy phenomenology of scalar leptoquarks at one-loop accuracy, J. High Energy Phys. 01 (2021) 138.

[114] D. Chakraverty, D. Choudhury, and A. Datta, A non-supersymmetric resolution of the anomalous muon magnetic moment, Phys. Lett. B **506**, 103 (2001).

[115] K.-m. Cheung, Muon anomalous magnetic moment and leptoquark solutions, Phys. Rev. D **64**, 033001 (2001).

[116] C. Biggio, M. Bordone, L. Di Luzio, and G. Ridolfi, Massive vectors and loop observables: The $g-2$ case, J. High Energy Phys. 10 (**2016**) 002.

[117] E. Coluccio Leskow, G. D'Ambrosio, A. Crivellin, and D. Müller, $(g-2)\mu$, lepton flavor violation, and Z decays with leptoquarks: Correlations and future prospects, Phys. Rev. D **95**, 055018 (2017).

[118] C.-H. Chen, T. Nomura, and H. Okada, Excesses of muon $g-2$, $R_{D^{(*)}}$, and R_K in a leptoquark model, Phys. Lett. B **774**, 456 (2017).

[119] D. Das, C. Hati, G. Kumar, and N. Mahajan, Towards a unified explanation of $R_{D^{(*)}}$, R_K and $(g-2)_\mu$ anomalies in a left-right model with leptoquarks, Phys. Rev. D **94**, 055034 (2016).

[120] A. Crivellin, M. Hoferichter, and P. Schmidt-Wellenburg, Combined explanations of $(g-2)_{\mu,e}$ and implications for a large muon EDM, Phys. Rev. D **98**, 113002 (2018).

[121] K. Kowalska, E. M. Sessolo, and Y. Yamamoto, Constraints on charmphilic solutions to the muon $g-2$ with leptoquarks, Phys. Rev. D **99**, 055007 (2019).

[122] I. Doršner, S. Fajfer, and O. Sumensari, Muon $g-2$ and scalar leptoquark mixing, J. High Energy Phys. 06 (2020) 089.

[123] I. Bigaran and R. R. Volkas, Getting chirality right: Single scalar leptoquark solutions to the $(g-2)_{e,\mu}$ puzzle, Phys. Rev. D **102**, 075037 (2020).

[124] I. Doršner, S. Fajfer, and S. Saad, $\mu \to e\gamma$ selecting scalar leptoquark solutions for the $(g-2)_{e,\mu}$ puzzles, Phys. Rev. D **102**, 075007 (2020).

[125] K. S. Babu, P. S. B. Dev, S. Jana, and A. Thapa, Unified framework for B-anomalies, muon $g-2$ and neutrino masses, J. High Energy Phys. 03 (2021) 179.

[126] A. Crivellin, D. Mueller, and F. Saturnino, Correlating h$\mu+\mu$- to the Anomalous Magnetic Moment of the Muon via Leptoquarks, Phys. Rev. Lett. **127**, 021801 (2021).

[127] D. Aristizabal Sierra, M. Hirsch, and S. G. Kovalenko, Leptoquarks: Neutrino masses and accelerator phenomenology, Phys. Rev. D **77**, 055011 (2008).

[128] D. Zhang, Radiative neutrino masses, lepton flavor mixing and muon $g-2$ in a leptoquark model, J. High Energy Phys. 07 (2021) 069.

[129] W. Buchmuller, R. Ruckl, and D. Wyler, Leptoquarks in lepton—quark collisions, Phys. Lett. B **191**, 442 (1987); **448**, 320(E) (1999).

[130] G. Valencia and S. Willenbrock, Quark—lepton unification and rare meson decays, Phys. Rev. D **50**, 6843 (1994).

[131] A. V. Kuznetsov and N. V. Mikheev, Vector leptoquarks could be rather light?, Phys. Lett. B **329**, 295 (1994).

[132] N. Assad, B. Fornal, and B. Grinstein, Baryon number and lepton universality violation in leptoquark and diquark models, Phys. Lett. B **777**, 324 (2018).

[133] A. Bhaskar, D. Das, T. Mandal, S. Mitra, and C. Neeraj, Precise limits on the charge-$2/3\times$ U_1 vector leptoquark, Phys. Rev. D **104**, 035016 (2021).

[134] J. M. Arnold, B. Fornal, and M. B. Wise, Phenomenology of scalar leptoquarks, Phys. Rev. D **88**, 035009 (2013).

[135] A. Bolaños, A. Moyotl, and G. Tavares-Velasco, Static weak dipole moments of the τ lepton via renormalizable scalar leptoquark interactions, Phys. Rev. D **89**, 055025 (2014).

[136] R. Mohanta, Effect of scalar leptoquarks on the rare decays of B_s meson, Phys. Rev. D **89**, 014020 (2014).

[137] B. Allanach, A. Alves, F. S. Queiroz, K. Sinha, and A. Strumia, Interpreting the CMS $\ell^+\ell^- jj E/_{\mathrm{T}}$ excess with a leptoquark model, Phys. Rev. D **92**, 055023 (2015).

[138] U. K. Dey and S. Mohanty, Constraints on leptoquark models from IceCube data, J. High Energy Phys. 04 (2016) 187.

[139] S. Sahoo and R. Mohanta, Leptoquark effects on $b \to s\nu\bar{\nu}$ and $B \to Kl^+l^-$ decay processes, New J. Phys. **18**, 013032 (2016).

[140] S. Baek and K. Nishiwaki, Leptoquark explanation of $h \to \mu\tau$ and muon $(g-2)$, Phys. Rev. D **93**, 015002 (2016).

[141] S. Sahoo and R. Mohanta, New physics effects in charm meson decays involving $c \to ul^+l^-(l_i^{\mp}l_j^{\pm})$ transitions, Eur. Phys. J. C **77**, 344 (2017).

[142] J.-H. Sheng, R.-M. Wang, and Y.-D. Yang, Scalar leptoquark effects in the lepton flavor violating exclusive $b \to s\ell_i^-\ell_j^+$ decays, Int. J. Theor. Phys. **58**, 480 (2019).

[143] R. Mandal and A. Pich, Constraints on scalar leptoquarks from lepton and kaon physics, J. High Energy Phys. 12 (2019) 089.

[144] K. Chandak, T. Mandal, and S. Mitra, Hunting for scalar leptoquarks with boosted tops and light leptons, Phys. Rev. D **100**, 075019 (2019).

[145] W. Dekens, J. de Vries, M. Jung, and K. K. Vos, The phenomenology of electric dipole moments in models of scalar leptoquarks, J. High Energy Phys. 01 (2019) 069.

[146] A. Crivellin, M. Hoferichter, M. Kirk, C. A. Manzari, and L. Schnell, First-generation new physics in simplified models: From low-energy parity violation to the LHC, J. High Energy Phys. 10 (2021) 221.

[147] S.-P. He, Leptoquark and vectorlike quark extended models as the explanation of the muon $g-2$ anomaly, Phys. Rev. D **105**, 035017 (2022); **106**, 039901(E) (2022).

[148] I. Bigaran and R. R. Volkas, Reflecting on chirality: CP-violating extensions of the single scalar-leptoquark solutions for the $(g-2)_{e,\mu}$ puzzles and their implications for lepton EDMs, Phys. Rev. D **105**, 015002 (2022).

[149] F. S. Queiroz, K. Sinha, and A. Strumia, Leptoquarks, dark matter, and anomalous LHC events, Phys. Rev. D **91**, 035006 (2015).

[150] S. Bansal, R. M. Capdevilla, A. Delgado, C. Kolda, A. Martin, and N. Raj, Hunting leptoquarks in monolepton searches, Phys. Rev. D **98**, 015037 (2018).

[151] S. Iguro, M. Takeuchi, and R. Watanabe, Testing leptoquark/EFT in $\bar{B} \to D^{(*)}l\bar{\nu}$ at the LHC, Eur. Phys. J. C **81**, 406 (2021).

[152] T. Husek, K. Monsalvez-Pozo, and J. Portoles, Constraints on leptoquarks from lepton-flavour-violating tau-lepton processes, J. High Energy Phys. 04 (2022) 165.

[153] D. Bečirević, I. Doršner, S. Fajfer, D. A. Faroughy, F. Jaffredo, N. Košnik, and O. Sumensari, Model with two scalar leptoquarks: R_2 and S_3, Phys. Rev. D **106**, 075023 (2022).

[154] A. Crivellin, B. Fuks, and L. Schnell, Explaining the hints for lepton flavour universality violation with three S_2 leptoquark generations, J. High Energy Phys. 06 (2022) 169.

[155] R. Aaij *et al.* (LHCb Collaboration), Test of lepton universality with $B^0 \to K^{*0}\ell^+\ell^-$ decays, J. High Energy Phys. 08 (2017) 055.

[156] R. Aaij *et al.* (LHCb Collaboration), Test of lepton universality in beauty-quark decays, Nat. Phys. **18**, 277 (2022).

[157] LHCb collaboration, Test of lepton universality in $b \to s\ell^+\ell^-$ decays, arXiv:2212.09152.

[158] P. Langacker, Parity violation in muonic atoms and cesium, Phys. Lett. B **256**, 277 (1991).

[159] L. Lavoura, General formulae for $f_1 \times \to f_{2\gamma}$, Eur. Phys. J. C **29**, 191 (2003).

[160] E. Gabrielli, Model independent constraints on leptoquarks from rare muon and tau lepton processes, Phys. Rev. D **62**, 055009 (2000).

[161] M. Leurer, New Bounds on Leptoquarks, Phys. Rev. Lett. **71**, 1324 (1993).

[162] E. Keith and E. Ma, Oblique S and T Parameters and Leptoquarks at HERA, Phys. Rev. Lett. **79**, 4318 (1997).

[163] A. Crivellin, D. Müller, and F. Saturnino, Leptoquarks in oblique corrections and Higgs signal strength: Status and prospects, J. High Energy Phys. 11 (2020) 094.
[164] J. K. Mizukoshi, O. J. P. Eboli, and M. C. Gonzalez-Garcia, Bounds on scalar leptoquarks from Z physics, Nucl. Phys. **B443**, 20 (1995).
[165] J. de Blas, M. Chala, M. Perez-Victoria, and J. Santiago, Observable effects of general new scalar particles, J. High Energy Phys. 04 (2015) 078.
[166] A. M. Sirunyan *et al.* (CMS Collaboration), Search for pair production of first-generation scalar leptoquarks at $\sqrt{s} = 13$ TeV, Phys. Rev. D **99**, 052002 (2019).
[167] G. Aad *et al.* (ATLAS Collaboration), Search for pairs of scalar leptoquarks decaying into quarks and electrons or muons in $\sqrt{s} = 13$ TeV pp collisions with the ATLAS detector, J. High Energy Phys. 10 (2020) 112.
[168] G. Aad *et al.* (ATLAS Collaboration), Search for pair production of scalar leptoquarks decaying into first- or second-generation leptons and top quarks in proton–proton collisions at $\sqrt{s} = 13$ TeV with the ATLAS detector, Eur. Phys. J. C **81**, 313 (2021).
[169] A. Tumasyan *et al.* (CMS Collaboration), Search for new particles in events with energetic jets and large missing transverse momentum in proton-proton collisions at $\sqrt{s} = 13$ TeV, J. High Energy Phys. 11 (2021) 153.
[170] ATLAS Collaboration, Search for pair-produced scalar and vector leptoquarks decaying into third-generation quarks and first- or second-generation leptons in pp collisions with the ATLAS detector, arXiv:2210.04517.
[171] A. Crivellin and L. Schnell, Complete Lagrangian and set of Feynman rules for scalar leptoquarks, Comput. Phys. Commun. **271**, 108188 (2022).
[172] G. Passarino and M. J. G. Veltman, One loop corrections for e^+e^- annihilation into $\mu^+\mu^-$ in the Weinberg model, Nucl. Phys. **B160**, 151 (1979).
[173] R. Mertig, M. Bohm, and A. Denner, FeynCalc: Computer algebraic calculation of Feynman amplitudes, Comput. Phys. Commun. **64**, 345 (1991).
[174] V. Shtabovenko, R. Mertig, and F. Orellana, FeynCalc 9.3: New features and improvements, Comput. Phys. Commun. **256**, 107478 (2020).
[175] H. H. Patel, Package-X: A *Mathematica* package for the analytic calculation of one-loop integrals, Comput. Phys. Commun. **197**, 276 (2015).
[176] A. M. Sirunyan *et al.* (CMS Collaboration), Search for Leptoquarks Coupled to Third-Generation Quarks in Proton-Proton Collisions at $\sqrt{s} = 13$ TeV, Phys. Rev. Lett. **121**, 241802 (2018).
[177] A. M. Sirunyan *et al.* (CMS Collaboration), Search for third-generation scalar leptoquarks decaying to a top quark and a τ lepton at $\sqrt{s} = 13$ TeV, Eur. Phys. J. C **78**, 707 (2018).
[178] G. Aad *et al.* (ATLAS Collaboration), Search for new phenomena in pp collisions in final states with tau leptons, b-jets, and missing transverse momentum with the ATLAS detector, Phys. Rev. D **104**, 112005 (2021).
[179] M. Schmaltz and Y.-M. Zhong, The leptoquark Hunter's guide: Large coupling, J. High Energy Phys. 01 (2019) 132.
[180] G. W. Bennett *et al.* (Muon $g-2$ Collaboration), Final report of the muon E821 anomalous magnetic moment measurement at BNL, Phys. Rev. D **73**, 072003 (2006).
[181] B. Abi *et al.* (Muon $g-2$ Collaboration), Measurement of the Positive Muon Anomalous Magnetic Moment to 0.46 ppm, Phys. Rev. Lett. **126**, 141801 (2021).
[182] T. Aoyama *et al.*, The anomalous magnetic moment of the muon in the Standard Model, Phys. Rep. **887**, 1 (2020).
[183] W. Altmannshofer *et al.* (Belle-II Collaboration), The Belle II physics book, Prog. Theor. Exp. Phys. **2019**, 123C01 (2019); **2020**, 029201(E) (2020).
[184] B. Aubert *et al.* (*BABAR* Collaboration), Searches for Lepton Flavor Violation in the Decays $\tau^\pm \to e^\pm\gamma$ and $\tau^\pm \to \mu^\pm\gamma$, Phys. Rev. Lett. **104**, 021802 (2010).
[185] G. J. van Oldenborgh, FF: A package to evaluate one loop Feynman diagrams, Comput. Phys. Commun. **66**, 1 (1991).
[186] T. Hahn and M. Perez-Victoria, Automatized one loop calculations in four-dimensions and D-dimensions, Comput. Phys. Commun. **118**, 153 (1999).
[187] A. Denner, S. Dittmaier, and L. Hofer, Collier: A Fortran-based complex one-loop library in extended regularizations, Comput. Phys. Commun. **212**, 220 (2017).
[188] G. Tavares-Velasco, https://github.com/gitavaresve/Top-QuarkDecay/tree/main, 10.5281/zenodo.7854286 (2023).